UiT
THE ARCTIC UNIVERSITY OF NORWAY

Faculty of Health Sciences, Department of Pharmacy

Synthesis of copper and silver nanoparticles with extracts of berries: A green chemistry approach

—

Christoffer J. Løkse

Master's thesis in Pharmacy May 2017

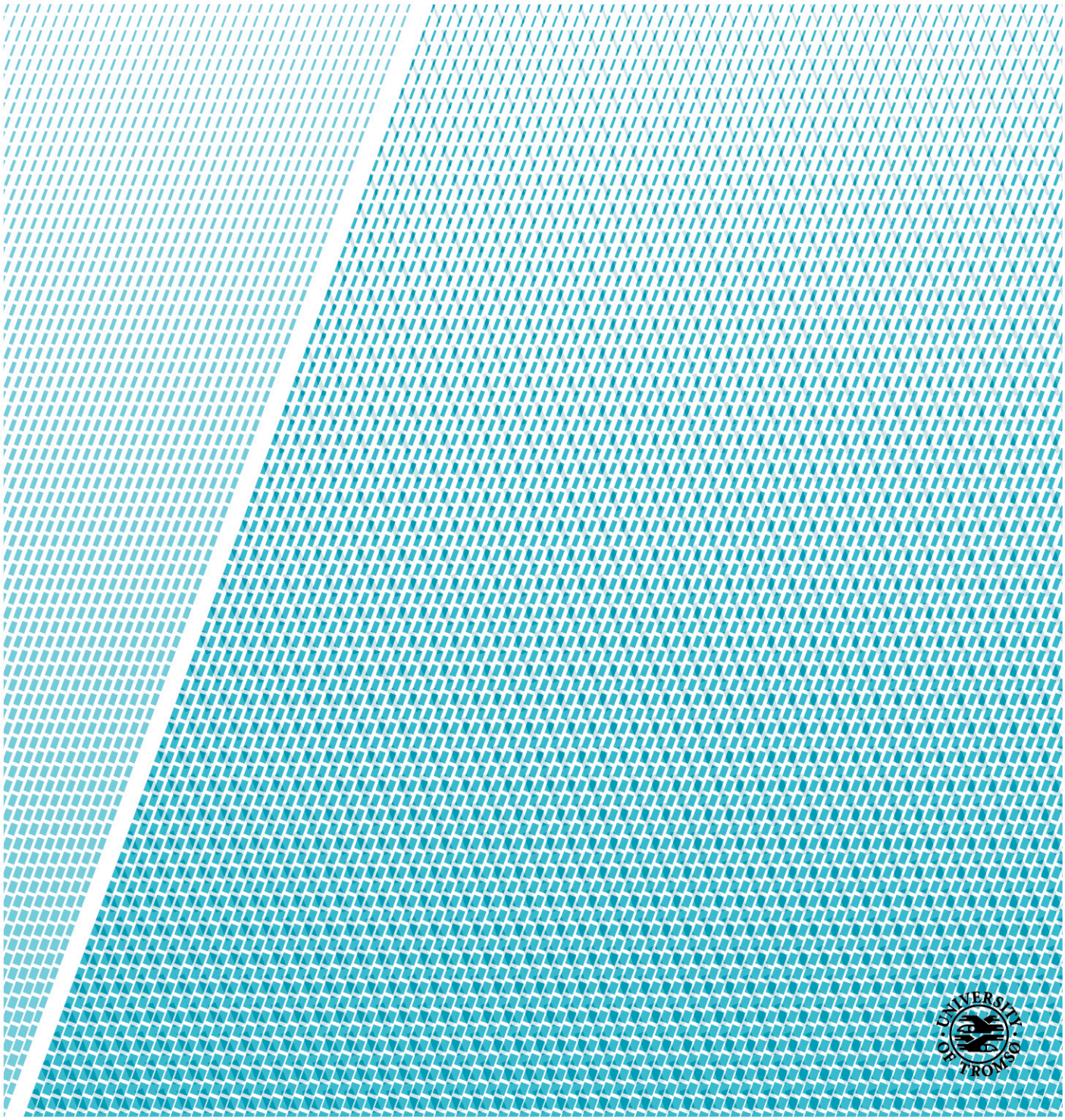

FOREWORD

The laboratory work presented in this thesis was performed at the Physical Chemistry Department and Biology Department at the University of Florence (UniFi).

Dr. Sandra Ristori at the Department of Physical Chemistry, UniFi, was the main supervisor. Professor Natasa Skalko-Basnet, Drug Transport and Delivery Research Group, Department of Pharmacy, was the internal supervisor at the University of Tromsø, UiT.

ACKNOWLEDGEMENTS

First, I would like to thank my supervisor Dr. Sandra Ristori at the University of Florence, who had the main responsibility for the practical laboratory work during my stay in Italy. Thank you for making my stay in Italy unforgettable. I am also very grateful for the help, advice and supervision of Professor Natasa Skalko-Basnet, even in times when panic and frustration took over.

I would also like to thank all the people that were collaborating with us, and who have also taken part in the work presented here. I am grateful for their efforts, their assistance and encouragement through the laboratory work: Enrico Casalone (Department of Biology), Massimo Del Bubba, Claudia Ancillotti (Department of Chemistry "Ugo Schiff"), Purusotam Basnet (University Hospital of Northern Norway, UNN). And, of course, to the students Emilia Benassai and Martino Pini, that were very helpful and supportive, especially when my time in Italy was coming to an end.

Of course, I would also like to thank the wonderful people I met during my stay, especially Felicia and Mattia. Thank you for the road trips, the food, the laughter, the madness and the company. Thank you for making my stay in Italy a memory for life.

To Sondre, for words of encouragement throughout the research and writing process of this thesis.

To Marion, for taking the time to come and visit me in Firenze, and for making it an unforgettable week.

A great thanks to the voices in my head, keeping me sane during my stay in Italy.

Finally, I would like to thank my family for their support and encouragement throughout my education. Without you I would most likely have become Batman.

Tromsø, May 2017

Christoffer Jacobsen Løkse

Table of Contents

SAMMENDRAG 1
ABSTRACT 2
LIST OF ABBREVIATIONS 3
1 INTRODUCTION 4
1.1 Metal nanoparticles from plant extracts 6
1.1.1 Green chemistry 6
1.1.2 Plant extracts 9
1.1.3 Copper nanoparticles from plant extracts 10
1.1.4 Silver nanoparticles from plant extracts 10
1.2 Characterization of nanoparticles 12
1.2.1 Transmission electron microscopy (TEM) 12
1.2.2 X-ray photoelectron spectroscopy 13
1.3 Evaluation of antimicrobial activity 14
1.3.1 Sensitivity assay 14
1.3.2 Agar diffusion testing 14
1.4 Toxicity evaluation 15
1.4.1 Cytotoxicity assay 15
2 AIMS OF THE STUDY 16
3 MATERIALS AND METHODS 17
3.1 Chemicals and solutions 17
3.2 Equipment 18
3.3 Plant extract preparation 19
3.4 Synthesis of metal nanoparticles at 70°C 20
3.4.1 First synthesis 20
3.4.2 Second synthesis 20
3.5 Synthesis of nanoparticles at 50°C 21
3.6 Purification of copper nanoparticles 22
3.7 Transmission electron microscopy analysis 22
3.8 X-ray photoelectron spectroscopy 22
3.9 Agar disk diffusion antibacterial testing 23
3.10 Antibacterial testing in tube with liquid medium 23
3.11 Sensitivity assays 24
3.12 Cytotoxicity assay 25
4 RESULTS AND DISCUSSION 26
4.1 Synthesis of metal nanoparticles at 70°C 26

4.1.1 First synthesis of copper nanoparticles at 70°C 26
4.1.2 Second synthesis of silver nanoparticles at 70°C 28
4.2 Synthesis of copper and silver nanoparticles at 50°C 29
4.3 Purification of copper nanoparticles 30
4.4 Transmission electron microscopy 31
4.4.1 TEM images of nanoparticle suspensions of $CuCl_2$ + M/G and $Cu(Ac)_2$ + M/G synthesised at 70°C 31
4.4.2 TEM images of purified nanoparticle suspensions of $CuCl_2$ + M/G and $Cu(Ac)_2$ + M/G synthesised at 70°C 35
4.4.3 TEM images of nanoparticle suspensions of $AgNO_3$ and $CuNO_3$ (0.0125M) nanoparticles + M/G (diluted 1:1, v/v) synthesised at 50°C 39
4.4.4 TEM images of nanoparticle suspensions of $AgNO_3$ at 0.025M with undiluted extract and $AgNO_3$ at 0.0125M with extract diluted 1:1. Synthesised at 70°C 42
4.5 X-ray photoelectron spectroscopy 48
4.6 Antimicrobial potential of nanoparticles 49
4.6.1 Agar diffusion testing 49
4.7 Antibacterial testing in tubes with liquid medium 51
4.8 Sensitivity assays 53
4.9 Cytotoxicity assay 54
5 CONCLUSION 57
6 FUTURE PERSPECTIVES 59
Reference list 60
Appendix 64

SAMMENDRAG

Nanopartikler er vanligvis definert som partikler i en størrelsesorden 1-100 nm, og disse partiklene har ofte andre egenskaper enn ikke-nano materiale med samme kjemiske komposisjon. I de seneste årene har interessen og bruken av nanopartikler økt, det samme har også interessen for å forstå partiklenes oppførsel, innvirkning og skjebne i miljøet. I de siste tiårene har det også vært spesielt fokus på søken etter mer øko-vennlige syntesestrategier, spesielt i farmasøytisk industri. De tre hovedområdene hvor prinsippene for grønn kjemi kan anvendes i syntesen av nanopartikler av metall er: "capping agent", reduksjonsmiddel og løsemiddel. Sammen med bruken av reagenser og løsemidler med lav toksisitet, er også lav energikonsumpsjon ønsket. Blåbærekstraktene (*V. myrtillus* og *V. gaultherioides*) er kjente reduksjonsmidler, og fungerer også som "capping-agent" i syntesen. Siden ekstraktene er vandige er det heller ikke behov for toksiske eller farlige løsemidler i syntesen. Selve syntesen foregår også under relativt lave temperaturer (50°C og 70°C), noe som også har positiv effekt på energikonsumpsjonen.

Hovedfokuset i denne studien var å anvende prinsippene for grønn kjemi i syntesen av metalliske nanopartikler av kobber og sølv, ved å bruke ekstrakt fra blåbær for å redusere metallforløperne i stedet for miljøskadelige og toksiske materialer. Bruken av verdifulle biprodukter fra landbruk bidrar også til en merverdi for storskalaproduksjon. Siden størrelse og struktur på de metalliske nanopartiklene har vist seg å være viktig for antimikrobiell effekt, ble størrelse og form karakterisert ved hjelp av transmisjonselektronmikroskopi (TEM). Det antimikrobielle potensialet av forskjellige typer nanopartikler ble sammenlignet og korrelert til produksjonsmetode. For å sikre anvendelighet av det utviklede systemet i behandling av hudinfeksjoner, ble cytotoksisiteten til nanopartiklene analysert i keratinocytter.

Vi klarte å syntetisere metalliske nanopartikler av kobber og sølv ved å bruke ekstrakt fra to arter av blåbær som reduksjonsmiddel, og størrelse og form av nanopartiklene ble karakterisert med TEM analyse. Selv om nanopartiklene av kobber ikke viste forventet antibakteriell effekt under forholdene anvendt i denne studien, viste nanopartiklene av sølv antibakteriell effekt, selv om effekten var lavere enn for saltløsningen med metallforløper alene. Dette kan muligens korreleres med at suspensjonene med nanopartikler ikke var stabile; nanopartiklene (og ekstraktet) aggregerte og sedimenterte tydelig under oppbevaring. Av mest sannsynlig samme grunn viste alle suspensjonene toksisitet mot keratinocytter ved alle konsentrasjoner testet i cytotoksisitetsanalysen.

For å kunne konkludere om de syntetiserte nanopartiklene faktisk er lovende antibakterielle midler, samt å bestemme tilsynelatende toksisitet, må videre eksperimentering utføres. Disse kan utføres ved å variere konsentrasjon av ekstrakt og metallforløper, eller ved å tilsette ikke-toksiske stabilisatorer som for eksempel citrat fra plantekilder, for å lage en nanopartikkel-suspensjon med lengre holdbarhet. Temperatur og røremetode under syntese kan også optimaliseres for å oppnå bedre stabilitet av suspensjonen.

ABSTRACT

Nanoparticles are usually defined as particles in a size range of 1-100 nm, and these particles often have different properties than the non-nanoscale material of the same chemical composition. In recent years, as the interest and use of nanoparticles has increased and so has the interest in understanding their behaviour, impact and fate in the environment. In the last decades, there has been special focus on the search for more eco-friendly synthesis strategies, especially in the pharmaceutical industry. The three main areas where the principles of green chemistry could be applied in the synthesis of metal nanoparticles are: the capping agent, the reducing agent and the solvent. Along with the use of reagents and solvents with low toxicity, a low power consumption is desirable. The blueberry extracts (*V. myrtillus* and *V. gaultheroides*) are the known reducing agents as well as the capping agents. Since the extract is aqueous there was no need for toxic or dangerous solvents to be employed in the synthesis either. Finally, the synthesises were performed at relatively low temperatures (50°C and 70°C), which also positively affects the power consumption.

The main aim of this study was to apply the principles of green chemistry on the synthesis of metallic copper and silver nanoparticles, using extract of blueberries to reduce the metal precursors instead of more environmentally damaging and toxic materials. Employing valuable agricultural by-products also represent an added value for large scale production. Since the size and structure of metal nanoparticles has been shown to be important for the antimicrobial effect, the nanoparticles size and shape were characterised by transmission electron microscopy (TEM). The antimicrobial potential of different types of nanoparticles were compared, and correlated to the manufacturing procedure. To assure the applicability of the developed system in treatment of skin infections, the cytotoxicity of nanoparticles was assayed in keratinocytes.

We managed to synthesise the copper and silver nanoparticles by using extracts of two different species of blueberry as a reducing agent and the size and structure of the metal nanoparticles were characterised by TEM analysis. Although the copper nanoparticles did not exhibit expected antibacterial effect under the conditions applied in our study, the silver nanoparticles did exhibit antibacterial effect, although less than detected for the metal precursor salt solution alone. This might be correlated to the fact that the nanoparticle suspensions were not stable; the nanoparticles (and extract) clearly aggregated and precipitated upon storage. Most likely for the same reason, all nanoparticle suspensions showed toxicity toward keratinocytes at all concentrations tested in the cytotoxicity assay.

To conclude whether the synthesised nanoparticles are indeed promising antibacterials, as well as address apparent toxicity, further experiments should be performed. These can be done by varying the concentration of extract and metal precursor or by non-toxic stabilizers, such citrate from other plant sources, in order to obtain nanoparticle suspensions with longer shelf-life. The temperature of synthesis and stirring method could also be optimized.

LIST OF ABBREVIATIONS

AR – Antibiotic resistance

Ag-NPs – Silver nanoparticles

Cu-NPs – Copper nanoparticles

$Cu(Ac)_2$ – $Cu(CH_3COO)_2$

FRAP – Ferric reducing antioxidant power

G – *V. gaultheroides*

gaultheroides – V. gaultheroides

M – *V. myrtillus*

myrtillus – V. myrtillus

MTT - 3-(4,5-dimethylthiazol-2-yl)-2,5-diphenyltetrazolium bromide

NP - Nanoparticle

ROS – Reactive Oxygen Species

RSA – Radical scavenging activity

TEM – Transmission Electron Microscopy

TMA – Total monomeric anthocyanins

TSP – Total soluble polyphenols

XPS – X-ray photoelectron spectroscopy

1 INTRODUCTION

Antibiotic resistance (AR) is becoming one of the greatest health challenges worldwide. The widespread use of antibiotic since the discovery of penicillin in 1928 has worked as an accelerator for the development of resistance. Up until the mid 1980s more than 25 new antibiotics were discovered or synthesised (1). The effectiveness of these drugs is reduced as more and more resistance occurs. Diseases that in the last decades have been easy to treat, will become more difficult to treat, or even become untreatable. Pneumonia, a disease that became easily treatable after the introduction of penicillin is getting more difficult to treat, which puts the lives of patients at risk. Common infections, surgical procedures, immunocompromised patients and neonatal will be at an increased risk of severe complications when antibiotics ceases to be effective. Antibiotic resistance can be defined as a microorganism's resistance against an antibiotic therapy that they originally were sensitive to. Today drug resistant bacteria are being treated by antibiotics in higher doses, administering several antibiotics and prolonging the treatments (2). This leads to increased toxicity and side effects, which again requires more supervision and treatment. This rapid increase of antibiotic resistance makes it necessary to search for alternative treatments, preferably treatments that do not cause, or are highly unlikely to cause, bacterial resistance(3). Vaccines could be an interesting approach, even though preventive vaccines against bacterial infections so far have limited applications (3, 4). Another strategy would be to enhance the activity of antibiotics that already exist. Some problems of antibiotic resistance might be bypassed by using nanoparticles to encapsulate antibiotics (5-7).

A promising approach against antibiotic resistance, that is already widely utilised, is based on finely divided metals, such as silver, gold or copper. Metallic nanoparticles (5-100 nm) are widely used in disinfection of drinking water, as wound dressings and for other antimicrobial purposes (2). There is still some concern about the prolonged exposure to nanoparticles of metals, although this seems to primarily apply to ions or salts of metals and not the metallic nanoparticles (e.g. Ag^0, Cu^0) (2, 8-10). However, nanoparticles may have an adverse effect on the environment (11-14). As far back as to the ancient Egyptians copper has been used as a biocide. It has been used to disinfect drinking water, wounds, prevent spreading of disease and treat skin diseases (15). In the mid 1700s copper (copper sulphate solution) was discovered to be an effective fungicide. Research done the last century has discovered that copper has antifungal, molluscicidal, antibacterial and antiviral properties (16). An interesting discovery is that bacteria exposed to metallic copper surfaces are completely inactivated, as opposed to entering a viable but non-cultivable physiological state (17). Even though copper has this effect on microorganisms it is considered safe for humans, and is, in fact, essential for normal human physiology and wound healing (18, 19). Copper ions (together with silver ions) are used for water treatment in hospitals, which is an important way to prevent the spread of infections (20). However, although copper has many positive and useful properties, it may be toxic to marine life and other organisms. Recently, major technological advancements have allowed us to obtain metallic copper (i.e. Cu^0) in the form of nanoparticles with a narrow size distribution and high uniformity. The production of copper nanoparticles (Cu-NPs) is less common than Ag or Au nanoparticles because of the lower reduction potential of copper, which facilitates re-oxidation from Cu^0 to CuO (and partially Cu_2O). However, when they are synthesized all these nanoparticles are rather toxic, and non-eco-friendly reagents are used in synthesis. Moreover, organic solvents are often used in the process of copper nanoparticle production (21).

Here it would be interesting to apply the principles of the so called “green chemistry and engineering” to develop a process that uses less toxic reagents and solvents, producing less toxic waste and byproducts with lower impact on human health and the environment. Preferably the process should also cost less than processes already in use today. Synthesis of Cu - NPs has already been performed using extracts from the leaves of the *Magnolia kobus* tree, making nanoparticles that had up to 99% antibacterial effect (22). Several other plant extracts have also been used for the synthesis of Cu-NPs, as well as for the synthesis of Au and Ag nanoparticles (23-27).

In this thesis, we applied the principles of green chemistry by using extracts from a perhaps even more readily available source: blueberries. The polyphenols found in the berries of *V. myrtillus L.* and *V. uliginosum L.* subsp. *gaultherioides* were used as a reducing agent in the synthesis of Cu-NPs. This allowed the use of water as solvent decreasing the use of non-eco-friendly ingredients further. Additionally, the synthesis was performed at lower temperatures (50-70°C), and in the perspective of a scalable process this will reduce the cost of the process even more. The green synthesis of Cu-NPs and the design and preparation of biocompatible vectors for the nanoparticles are an interesting approach to a more eco-friendly solution to antibiotic resistance.

1.1 Metal nanoparticles from plant extracts

Nanoparticles are usually defined as particles with a size around 1-100 nm (28). These particles often have different properties than the non-nanoscale particles of the same chemical composition (see Figure 1) (29). As the interest and use of nanoparticles has increased, so too has the interest in understanding their behaviour, impact and fate in the environment (28, 29).

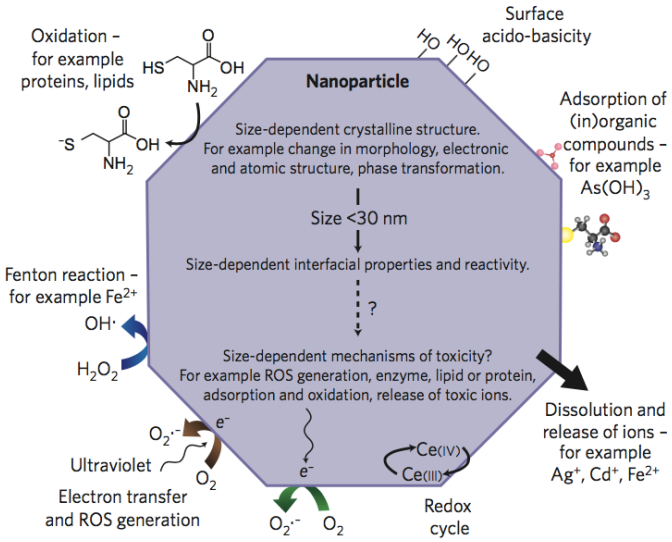

Figure 1 - A number of physiochemical mechanisms can occur at the surface of an inorganic nanoparticle. The potential relationship between the size dependence of the crystalline structure of nanoparticles (typically <30 nm), their interfacial properties (for example dissolution, oxidation, adsorption/desorption, electron transfer, redox cycles, Fenton reactions and surface acido-basicity) and potential mechanisms of toxicity (for example, the generation of ROS, the release of toxic ions, the oxidation of proteins and the adsorption of pollutants). OH·, hydroxyl radical; O2·-, anion superoxide. Figure and caption from Auffan et al. (29)

1.1.1 Green chemistry

In the last twenty years there has been more focus on the search for more eco-friendly synthesis strategies, especially in the pharmaceutical industry (30). Green chemistry and green engineering has been strongly encouraged by the international community (31). Applying the principles of green chemistry (32) to the synthesis of metal nanoparticles, we pay particular attention to three main factors: The capping agent, the reducing agent and the solvent. The use of reagents and solvents with low toxicity and low power consumption is desired. To guide the growth and morphology and give stability to the nanoparticles, capping agents are used. The most used capping agents are long hydrocarbon chain with heteroatoms, such as oleylamine (OAm), a primary alkyl amine that acts as an electron donor at higher temperatures and has affinity for metals through the NH_2 functional group; Dimethyldodecylamine, which presents acute toxicity with oral intake, skin contact and inhalation, and has a harmful effect to the aquatic environment; Troctylphosphine which is irritating to eyes and corrosive upon skin contact (33). Because of their toxicity, they should be removed before nanoparticles can be used for any further applications. In addition, some polymers, dendrimers and polysaccharides are used as capping agents.

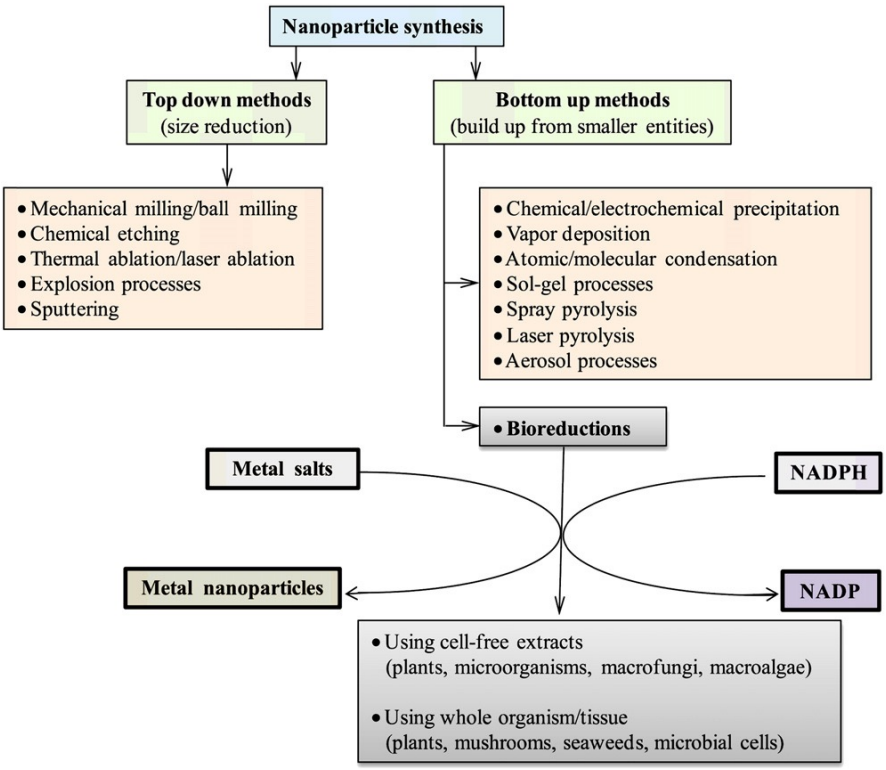

Figure 2 - Various approaches for making nanoparticles and cofactor dependent bioreduction. Figure and caption from Mittal et al. (27).

The reduction process is a fundamental step in the synthesis of nanoparticles. The commonly used reducing agents are sodium borohydride (NaBH4), hydrazine (N2H4) and formaldehyde. All of these reagents are toxic and polluting for the environment. Other organic molecules of vegetable origin may however be used as efficient reducing agents and at the same time be sustainable for the environment. Polysaccharides, for example, which react with the metals through the hydroxyl groups and have a very low cytotoxicity. Other types of plant-derived molecules known for antioxidant effects, such as the polyphenols content in many small fruits, including blueberries of the species *Vaccinium myrtillus L.* and *Vaccinium uliginosum L.* subsp. *gaultherioides,* can be used. These molecules are weaker reducing agents than those commonly used, but since they are water-soluble they allow complete dispersion in water.
The organic solvents normally used in the synthesis of nanoparticles are toxic for the operator, difficult to separate from the nanoparticles after synthesis and they require complex and expensive disposal procedures. Water, however, is non-toxic, non-flammable and has economic advantages.

Together with performing theses synthesises at low temperatures green chemistry will be better for the operators, the environment and more economically advantageous, especially when applied at an industrial scale.

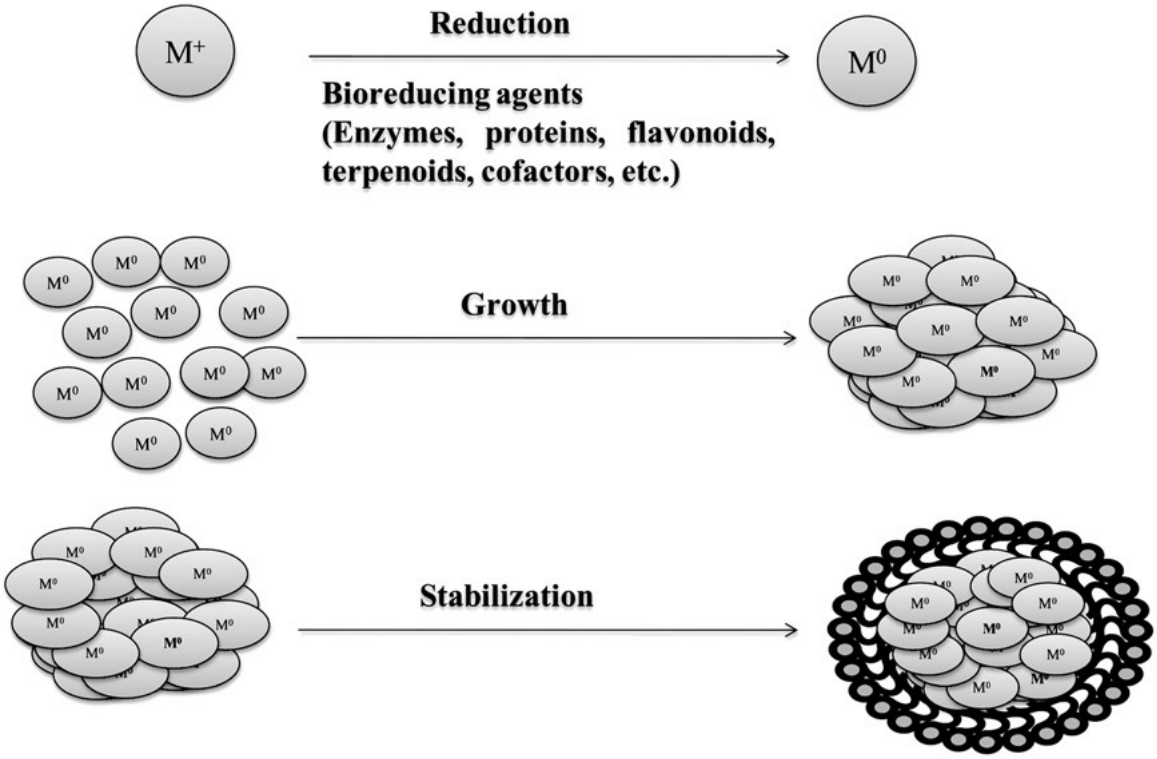

Figure 3 – Mechanism of nanoparticle synthesis (M^+ = metal ion). Figure and caption from Mittal et al. (27)

1.1.2 Plant extracts

For this study, aqueous extracts obtained from different species of wild and cultivated berries were used: *V. myrtillus L.* and *V. uliginosum L.* subsp. *gaultherioides.*

Figure 4 – *V. myrtillus* (left) and *V. gaultherioides* (right) (34, 35)

V. myrtillus is a local resource that is used not only as food, but as a supplement because of the high content of antioxidants. *V. gaultherioides* is also called "false blueberry" because of its similarity to blueberries yet has a much less palatable taste. These two species have different compositions of substances, polyphenols, contained in the fruit. The composition of total soluble polyphenols (TSP), total monomeric anthocyanins (TMA), radical scavenging activity (RSA) and ferric reducing antioxidant power (FRAP) of the blueberries used in this thesis have previously been analysed by Ancilotti et al.(36). This data (Table 1) shows that the *V. myrtillus* had the highest values of TSP, TMA, RSA and FRAP. They also contained more of the polyphenol class anthocyanines. This group includes the phenolic compound with the strongest reduction power, delphinidine, which also seem to exist at higher concentrations in *V. myrtillus* compared to *V. gaultherioides* (36, 37).

Table 1 - Composition of TSP, TMA, RSA and FRAP in *V. myrtillus* and *V. gaultheroides* gathered autumn 2015 (36).

Species	**Total Polyphenols** (mg catechin eq g^{-1} dw)	**Total monomeric anthocyanins** (mg cyanidin-3-glucoside eq g^{-1} dw)	**Antiradical activity** (µg DPPH mg^{-1} dw)	**Antioxidant activity** (mg Trolox eq g^{-1} dw)
V. myrtillus	33.5 ± 6.0	26.8 ± 4.5	154 ± 27	132 ± 14
V. gaultherioides	25.6 ± 3.4	12.3 ± 2.2	113 ± 23	95 ± 14

1.1.3 Copper nanoparticles from plant extracts

A "green" method for the synthesis of copper nanoparticles is by the reduction of the metal salt precursor in an aqueous phase with plant extracts (23). However, as mentioned above, the copper metal of the nanoparticles often has a high tendency to oxidize, which makes it a less stable product compared to what one would get by using metals such as gold and silver. The standard reduction potentials of gold, silver and copper in solution are:

$AuCl_4$ - (aq) + 3 e^- → Au (s) + 4 Cl (aq), E° (V) = 1.00

Ag^+ (aq) + e^- ⇔ Ag (s), E° (V) = 0.7996

Cu^{2+} (aq) + 2 e^- → Cu (s), E° (V) = 0.337

The standard reduction potential of gold is much lower than that of copper; it is therefore easier for the gold to be reduced, while it is easier for copper to undergo the reverse process, oxidation. To obtain metallic copper nanoparticles a reducing agent with an adequate reduction potential, less than 0.337 V, must be used.

Voltammetry studies have been done on polyphenols in acetonitrile, which have shown a correlation between the number of hydroxyl groups bound to the B ring of a polyphenol, and the reducing power (38). An increase in OH groups led to an increase in reducing power. Another voltammetry study on polyphenols found in the plant *Vitis vinifera* showed an increase in reduction power as the pH increased from 3.5 to 7.0 (37). From these studies, it appears that the phenolic compound class with the strongest reduction power is delphinidine. This polyphenol should be abundantly present in *V. myrtillus* fruit (36). It must, however, be considered that the reduction potential of these types of molecules appear highly variable and dependent upon conditions such as solvent and pH (37).

1.1.4 Silver nanoparticles from plant extracts

The use of silver ions, metallic silver and silver nanoparticles is being investigated for use in burn and wound treatment, water treatment, fabrics and other areas (39). They also show low toxicity against human cells, high thermal stability and low volatility (39, 40). There is some concern that high or prolonged exposure to silver will lead to agyrosis and argyria, which causes permanent discolouration of skin and organs as well as possible decrease in kidney function and eyesight, and liver toxicity (41-43).

Silver nanoparticles has been shown to be superior against bacterial strains of *S. aureus* and *E. coli* compared to copper nanoparticles (44-46). The antibacterial mechanism of action is believed to be binding to thiol groups in the respiratory enzymes of the cell. It binds to the cell wall and membrane, inhibiting the respiration process (40). Silver ions are also antibacterial, but their mechanism of action is not fully understood. It is suggested that when silver ions enter the cell they turn the DNA molecule to its condensed form, stopping replication, which then leads to cell death (47, 48). Silver nanoparticles show greater antibacterial effect because of their extremely large surface area that gives a much better contact with microorganisms. The silver nanoparticles (Ag-NPs) bind to proteins in the cell

membrane and also penetrate inside the organism. The Ag-NPs interact with thiol groups in proteins, inhibiting cell division, which leads to cell death. Some of the metallic Ag-NPs release ions, which further increases antibacterial activity (48-50). According to Castellano (51) metallic silver is chemically inert, but when it comes in contact with moisture, as for example when in contact with skin when in a wound dressing, it is ionised and exhibits an antibacterial effect. Metallic silver in nanoparticle form makes this process go much faster, increasing amount of silver ions released, giving an increase in toxic effects.

Many different plant extracts have been used to synthesise silver nanoparticles before, as listed in a review by Prabhu and Poulose (42).

1.2 Characterization of nanoparticles

Nanoparticles are primarily characterized for their size and surface properties. There are different methods available to determine the size of nanoparticles; in this project, we focused on transmission electron microscopy. This technique is particularly suited for inorganic (i.e. oxides or salts) nanoparticles, which are not deformed by the drying process in sample preparation. X-Ray photoelectron spectroscopy was also performed on the suspensions with $CuCl_2$ and $Cu(Ac)_2$ as metal precursors. This was done to further verify the synthesis of metallic nanoparticles, and if possible, quantify the amount of metallic nanoparticles compared to CuO and unreacted salt of the copper precursor.

1.2.1 Transmission electron microscopy (TEM)

The transmission electron microscope is an instrument that works under high vacuum, by sending a beam of electrons, coming from a source such as a tungsten filament, toward the sample. The sample is placed on a standard TEM 3.05mm diameter grid ring. The electrons interact with the sample as they pass through it and this interaction forms an image, which is then magnified and focused onto a fluorescent screen placed below. TEM generally has a resolution of about 0.2 nm. Heavy metals, such as gold and copper, are visible with a good contrast compared to the organic component of the plant extract.

Normally biological samples are fixated by embedding it in a plastic or by using a negative staining material, in order to withstand the vacuum and to facilitate handling. Negative staining has been used for study and identification of lipid aggregates (like liposomes) in aqueous solutions (52). This sample pre-treatment is not necessary for metal nanoparticles, thus allowing much less artifacts to affect the measurement.

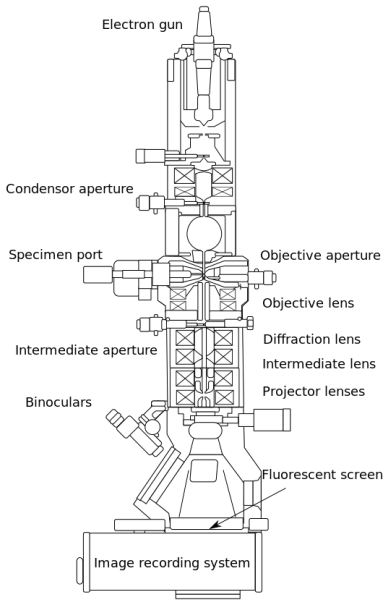

Figure 5 - Diagram outlining the internal components of a basic TEM system (53)

1.2.2 X-ray photoelectron spectroscopy

The XPS technique uses a source that emits a monochromatic X-ray beam, which then interacts with the atoms of the sample placed on the support, causing the emission of electrons. An electron collection lens collects these electrons. The emitted electron has a kinetic energy that depends on the energy of the x-ray radiation and energy of binding that it had with the nucleus of the atom:

$$E_b = h\upsilon - (E_k - \Phi)$$

E_b is the binding energy, $h\upsilon$ is the energy of x-ray photons, E_k is the kinetic energy of the electron and Φ is the work function of the instrument.

Once electrons are separated according to their kinetic energy, it is possible to determine the binding energy with the atom from which they were expelled. This is therefore a very sensitive and quantitative technique, which allows us to identify the various atomic species present in a sample, but also the degree of oxidation in which they are present and, based on the signal intensity, even in what quantity.

The supports, on which the samples are placed, can be of various materials. To analyse the copper samples a gold support was used and because of the vacuum it was cooled with liquid nitrogen. Gases and solvents trapped in the sample tend to be evaporated when under vacuum, which reduces the vacuum in the machine and making it impossible to complete the scan.

1.3 Evaluation of antimicrobial activity

1.3.1 Sensitivity assay

A sensitivity assay, or broth microdilution method, can be carried out to evaluate the sensitivity of a bacterial culture to an antibacterial sample (54). The assay can be carried out in a microtiter plate by incubation of a bacterial strain in the presence of two-fold dilution of the nanoparticles preparation. The wells are filled with a defined amount of inoculum, medium and antibacterial sample. Then it is diluted exponentially column 1 till 11, the wells in column 12 are used for positive and negative controls.

The minimum inhibitory concentration (MIC), defined as the lowest concentration of a sample that still shows inhibition on the growth of the bacteria (55), can be determined by performing a sensitivity assay. The MIC can be used to quantitatively measure the antibacterial activity of nanoparticles from plant extract.

1.3.2 Agar diffusion testing

Also referred to as disk diffusion sensitivity testing, is a way to test to what extent a bacterium is affected by an antibiotic (56). Small round paper plates are infused with a sample or an antibiotic and placed on an agar plate where the bacterium has been spread. It is then left to incubate overnight. If the sample kills or inhibits the bacterium, there will be an area around the disk where there is no visible growth of bacteria. This area is called the zone of inhibition. The diameter of the zone of inhibition tells us how strong the antibacterial effect is. A strong antibiotic will create a large circle, since a lower concentration is needed to inhibit growth or kill the bacteria.

1.4 Toxicity evaluation

Since silver, and in recent years also copper, have been used in wound dressings or the disinfect wounds (23, 40, 51), it was decided to test the cytotoxicity of nanoparticles in keratinocyte culture to assure the applicability of developed system in treatment of skin infections.

1.4.1 Cytotoxicity assay

To test the toxicity of the metal nanoparticles a MTT (3-(4,5-dimethylthiazol-2-yl)-2,5-diphenyltetrazolium bromide) based colorimetric assay was used. This assay is based on the cleavage of MTT from a yellow tetrazolium salt to purple formazan crystals, by metabolically active cells (57-59). This metabolization of MTT is due to the pyridine nucleotide cofactors NADH and NADPH (60). The purple formazan crystals that are formed are solubilized, colouring the solution, which is then quantified by a microplate reader.

2 AIMS OF THE STUDY

The aim of this study was to apply the principles of green chemistry on the synthesis of metallic copper and silver nanoparticles, using extract of blueberries to reduce the metal precursors.

Since size and structure of metal nanoparticles has been shown to be important for the antimicrobial effect, the nanoparticles size and shape were characterised by transmission electron microscopy.

Moreover, we compared the antimicrobial potential of different types of nanoparticles and prepared from different blueberry extracts.

Finally, the cytotoxicity of nanoparticles was assayed in keratinocyte culture to assure the applicability of developed system in treatment of skin infections.

3 MATERIALS AND METHODS

3.1 Chemicals and solutions

Table 2 – List of chemicals

Preparation of berry extract	**Synthesis of copper and silver nanoparticles**	**Sensitivity assay**
• Distilled H_2O • Ethanol-water 80/20 (v/v) solution with 2mM NaF • Freeze-dried *V. myrtillus* and *V. gaultherioides* berries • Ice for water bath	• Berry extract • Distilled/Sterile H_2O • $CuCl_2$ • $Cu(Acetate)_2$ • $CuNO_3$ • $AgNO_3$	• *E. coli* ATCC 35218 • *S. aureus* ATCC 29213 • *S. aureus* ATCC 25923 • Luria Bertani (LB) broth medium • LB agar • Ampicillin 1 mg/ml solution • NaCl 0.9% (w/v) solution •
Cytotoxicity assay		
• Cell Proliferation Kit I (MTT) from sigma-aldrich • Culture medium; ROMI 1640 containing 10% heat inactivated FCS (fetal calf serum), 2 mM glutamine and 1µg/mL actinomycin C_1 (actinomycin D).		

3.2 Equipment

Table 3: List of equipment

Analytical balance	-
Centrifuge	-
Heating plate/magnetic stirrer	-
Vortex mixer	-
Autoclave	
Spectrophotometer	Nach
Tubes for spectrophotometer	-
Modified glass tubes (light bulb shape)	-
Agar plates	-
Microtiter plates	-
BioPhotometer	Eppendorf
Microplate reader	TECAN infinite m200 PRO
Transmission Electron Microscope	TEM CM12 PHILIPS

3.3 Plant extract preparation

Freeze-dried samples of the whole fruit of *V. myrtillus L.* and *V. uliginosum L.* subsp. *gaultherioides* were used. The berries had been picked from 10 (*myrtillus*) and 11 (*gaultherioides*) different areas in Tuscany. An "average sample mix" was prepared by taking 1.0 g of sample from each area and mixing them, this mix of berries was then used for extract preparation. Approximately 2.0 g of sample of *V. myrtillus L.* and *V. gaultherioides* was weighed. These were each placed in two different flasks with a magnet bar for stirring. 60 mL of extraction solution, a mixture of ethanol/water 80/20 (v/v) containing 2.0 mM of NaF, was added to each. Sodium fluoride was used to inhibit polyphenol oxidase, an enzyme found in most fruits that oxidises the polyphenols, rendering them unable to reduce the copper ions from 2+ to 0. The samples were then stirred for 15 minutes in an ice bath, covered from light. Afterwards the samples were centrifuged for 5 minutes at 5000 rpm. The supernatant (extract) was decanted and stored; additional 60 mL of the extraction mixture was added to the pellet and the extraction process repeated one more time. The extraction solutions were afterwards placed in a rotary evaporator, to remove the ethanol. From 120 mL of solution, 24 mL of ethanol free solution was obtained. After ethanol was removed, the extract was filtered first through a 1.0 μm filter and then a 0.22 μm filter. This way the seeds and other solid parts are removed, as well as sterilising the extract.

For the next synthesises, extract was prepared with 1.5 g of freeze-dried berry and two extractions with 45 mL of extraction solution. From 90 mL of solution, 18 mL of ethanol free solution was obtained.

3.4 Synthesis of metal nanoparticles at 70°C

3.4.1 First synthesis

Four samples were prepared by adding 2.0 mL of metallic precursor (0.25 M solutions of $CuCl_2$ and $Cu(CH_3COO)_2$) to 18 mL of the extracts of *V. myrtillus* (M) and *V. gaultherioides* (G). Two "blank" samples, containing only the extracts, were prepared as controls.

Table 4 - Overview of samples for first synthesis

	Sample composition
1	2.0 mL 0.25 M $CuCl_2$ + 18.0 mL *myrtillus* extract
2	2.0 mL 0.25 M $Cu(CH_3COO)_2$ + 18.0 mL *myrtillus* extract
3	2.0 mL 0.25 M $CuCl_2$ + 18.0 mL *gaultherioides* extract
4	2.0 mL 0.25 M $Cu(CH_3COO)_2$ + 18.0 mL *gaultherioides* extract
5	20.0 mL *myrtillus* extract
6	20.0 mL *gaultherioides* extract

For the first 2 hours, the tubes were heated at ~ 70 °C in a water bath covered from light with aluminium foil. A magnet stirrer was used during the whole synthesis. The temperature was monitored throughout the synthesis with a thermometer. The temperature oscillated between 69 and 71 °C. After the first two hours, the heating was turned off and the stirring continued at room temperature (~ 20-25 °C) for an additional 22 hours (total time for synthesis 24 hours).

3.4.2 Second synthesis

For the second synthesis at 70°C silver nitrate solution was used in two different concentrations: 0.25M and 0.125M.

Table 5 - Overview of samples prepared for second synthesis

	Sample composition
1	1.0 mL 0.25 M $AgNO_3$ + 9.0 mL *myrtillus* extract
2	1.0 mL 0.25 M $AgNO_3$ + 9.0 mL *gaultherioides* extract
3	1.0 ml 0.125 M $AgNO_3$ + 4.5 mL *myrtillus* extract + 4.5 mL distilled H_2O
4	1.0 mL 0.125 M $AgNO_3$ + 4.5 mL *gaultherioides* extract + 4.5 mL distilled H_2O
5	5.0 mL *myrtillus* extract
6	5.0 mL *gaultherioides* extract

The synthesis itself was performed as described for the previous synthesis; the only difference was that the stirring for 22 hours was not performed to reduce the time of the synthesis.

3.5 Synthesis of nanoparticles at 50°C

For the synthesis at 50°C the following samples were prepared:

Table 6 - Overview of samples prepared for third synthesis

#	Sample compostition
1	1.0 mL 0.125 M $CuNO_3$ + 4.5 mL H_2O + 4.5 mL *myrtillus* extract
2	1.0 mL 0.125 M $AgNO_3$ + 4.5 mL H_2O + 4.5 mL *myrtillus* extract
3	1.0 mL 0.125 M $CuNO_3$ + 4.5 mL distilled H_2O + 4.5 mL *gaultherioides* extract
4	1.0 mL 0.125 M $AgNO_3$ + 4.5 mL distilled H_2O + 4.5 mL *gaultherioides* extract
5	5.0 mL *V. myrtillus* extract + 5.0 mL distilled H_2O
6	5.0 mL *gaultheroides* extract + 5.0 mL distilled H_2O

The synthesis was performed in a heating chamber at 50°C on an orbital shaking machine using sterilised glass beads as agitators inside the tubes. The samples were shaken for 2 hours. After the 2 hours, the heat and shaking was turned off, and the samples were kept still and protected from light overnight.

3.6 Purification of copper nanoparticles

A washing was performed by putting 1.0 mL of synthesised nanoparticle suspension ($CuCl_2$ + G, $CuCl_2$ + M, $Cu(CH_3COO_2)_2$ + G and $Cu(CH_3COO_2)_2$ + M) into 10 eppendorf tubes.

1. These tubes were then centrifuged at 15 000 rpm for 10 minutes.
2. The supernatants were decanted into another container and the pellet was re-suspended in 1.0 mL of a 1.0 M citric acid solution.
3. The tubes were centrifuged again at 15 000 rpm for 10 minutes
4. Supernatants were decanted into a new container and the pellets were re-suspended in 1.0 mL of 1.0 M citric acid solution
5. Then the tubes were centrifuged again at 15 000 rpm for 10 minutes
6. The supernatants were decanted into a new container
7. Pellets were re-suspended in distilled water (MilliQ) to remove the citric acid.
8. The samples were then centrifuged one last time at 15 000 rpm for 10 minutes.
9. Supernatants were decanted into a new container.
10. The pellets were then suspended in 1.0 mL of MilliQ water. The pellet in two of the eppendorf tubes of each sample were suspended in only 0.5 mL of MilliQ water, as to make 2 times the original concentration of nanoparticles. 1 tube of each sample was not re-suspended in water, in order to ease the lyophilisation before XPS analysis.

3.7 Transmission electron microscopy analysis

All samples containing nanoparticles and metal precursor were analysed by TEM. A small drop of sample was put on a standard TEM 3.05mm diameter grid ring, the liquid was evaporated and the grid was then inserted into the TEM. Four to eight images were taken of each sample to assure a representative sample. The machine used was TEM CM12 PHILIPS, equipped with an OLYMPUS Megaview G2 camera, at accelerating voltage of 100 keV.

3.8 X-ray photoelectron spectroscopy

The Eppendorf tubes from the purification process where the pellet had not been re-suspended were lyophilized as preparation for the XPS analysis. Samples were put on a gold plate support and analysed.

3.9 Agar disk diffusion antibacterial testing

As a way of testing antibacterial activity of the samples of the first nanoparticle synthesis ($CuCl_2$ and $Cu(Ac)_2$), an agar disk diffusion antibacterial test was performed (56). *S. aureus* or *E. coli* cells were spread on Luria Bertani (LB) agar plates (10 g bacto-tryptone, 5 g yeast extract, 10 g NaCl and 15 g technical agar per liter medium) (61, 62) with the help of sterile glass beads, to form a uniform bacterial lawn. Afterwards, six, standard, sterile paper disks were placed evenly spaced from each other on the agar plates, then 20 µL of sample was carefully dripped onto the disk. The plates were then incubated overnight at 37^{o}C. The day after the diameter of the zone of inhibition was measured to qualitative compare the antimicrobial activity of different samples.

3.10 Antibacterial testing in tube with liquid medium

To test the samples´ antibacterial activity suspended in a liquid medium, as opposed to when it is allowed to precipitate in the microtiter plate or only diffuse through a paper disk and agar, a liquid medium antibacterial test was performed:

Sterile plastic tubes (15 mL), each containing 1,0 mL of LB medium at 1.5x concentration, 0.1 mL of bacterial solution (*S. aureus* ATCC 29213 that was pre-inoculated a day in advance) and 0.35 mL of sample, were prepared. One additional tube was prepared with ampicillin (1µg/mL) as a positive control. LB 1.5x medium composition: 15 g bacto-tryptone, 7.5 g yeast extract and 15 g NaCl per liter medium.(61)
After incubation overnight, 10 µL was taken from the tubes and diluted in sterile NaCl 0.9% solution up to 1 mL, then 100 µL was spread on a LB agar plate and left to incubate overnight. The day after, the colonies on the plates were counted to determine the viability of the bacterial culture and compare the antimicrobial activity of different samples.

3.11 Sensitivity assays

One strain of *E. coli* and one strain of *S. aureus* were cultured in Luria Bertani (LB) broth. The broth contains 10g bacto-tryptone, 5g yeast extract and 10g NaCl per liter. The bacteria were incubated at 37°C on an orbital shaker (130 rpm) overnight. Afterwards the bacterial culture was diluted 10 times in a saline solution and OD_{600nm} was recorded and adjusted to reach OD_{600nm} = 0.2. A BioPhotometer (Eppendorf), zeroed against saline solution, was used to record the absorbance.

Round bottomed, transparent, 96 well (8x12) microtiter plates were used for the sensitivity assay. First all the wells in the plate were first filled with 50 µL of LB using a multi-channel pipette. For each sample, 50 µL of undiluted suspension was put into 1A-H wells and mixed 5 times (for this a single-channel pipette was used, changing tip for each different sample). Then using a multi-channel pipette w/o changing tips, 50 µL from wells 1A-H was withdrawn and transferred to the 2A-H wells and mixed 5 times, this was then repeated for the whole plate until the 11A-H wells; after the mixing 50 µL were removed from the 11A-H wells. The 12A-H wells were used as positive and negative control, and as chemicals sterility control or to see the OD of the samples alone (the samples with containing extracts had a very overpowering colour). The plates were then incubated for 24 h at 37^{o}C. A TECAN infinite m200 PRO microplate reader was used to read the OD600 nm: Mode: Absorbance, wavelength: 600 nm, bandwidth: 9 nm, number of flashes: 25, settle time: 0 ms.

3.12 Cytotoxicity assay

A Cell Proliferation Kit I (MTT) from Sigma-Aldrich was used to test the toxicity of the metal nanoparticles and controls. The cytotoxicity assay procedure for Cat. No. 11 465 007 001 was followed:

Table 7 - Procedure for cytotoxicity assay

Step	Action
1	WEHI-164 cells were preincubated at a concentration of $1*10^6$ cells/mL in culture medium with 1µg/mL actinomycin C1 for 3 hours at 37°C and 5-6.5% CO_2.
2	Cells were seeded at a concentration of $5*10^5$ cells/well in 100 µL culture medium containing 1 µg/mL actinomycin C_1 and various amounts of sample (1 µL, 5 µL and 10 µL) into tissue culture grade, 96 wells, flat bottom microplates. Blank = 100 µL medium Control = 90 µL cell suspension + 10 µL medium Sample = 90, 95 or 99 µL cell suspension + 10, 5 or 1 µL sample
3	Cell cultures were incubated for 24 hours at 37°C and 5-6.5% CO_2.
4	After incubation 10 µL of MTT labelling agent was added to each well (final concentration of 0.5 mg/mL).
5	The microplates were then incubated for 4 hours in a humidified atmosphere (37°C and 5-6.5% CO_2).
6	110 µL of the Solubilization solution was added to each well.
7	The plates were then allowed to stand overnight in the incubator in a humidified atmosphere (37°C and 5-6.5% CO_2).
8	The purple formazan crystals were checked for complete solubilisation and the spectrophotometric absorbance of the samples was measured using a microplate reader.

4 RESULTS AND DISCUSSION

4.1 Synthesis of metal nanoparticles at 70°C

The synthesis procedure used here is similar to most procedures involving plant extract in the synthesis of metal nanoparticles (22, 27, 63). This is a bottom up synthesis; where the nanoparticles are formed by the joining of smaller entities (27).

4.1.1 First synthesis of copper nanoparticles at 70°C

The setup of the synthesis is shown in Figure 6. The colour of the samples changed very little when adding the metal precursors, becoming slightly darker purple, which might be expected considering the blue colour of the metal precursor solution. The difference in extract colour between the *gaultherioides* and *myrtillus* extract is also very noticeable; the *myrtillus* has a much stronger and "blueberry-like" colour, while *gaultherioides* is more transparent and less purple. The samples containing the metal precursor $Cu(CH_3COO)_2$ had bit darker colour. No apparent change in colour from the start of the synthesis till the end was detected. One might have expected a slight shift towards a more copper metal (redish-yellow-brown) colour, as more and more copper ions were reduced to metallic Cu-NPs (64). After the end of the synthesis the samples were stored in a refrigerator at around 5°C. After overnight storage in the refrigerator, a dark precipitate was seen in the bottom of the tubes. This could indicate that the suspended Cu-NPs are not stable in suspension and tend to aggregate.

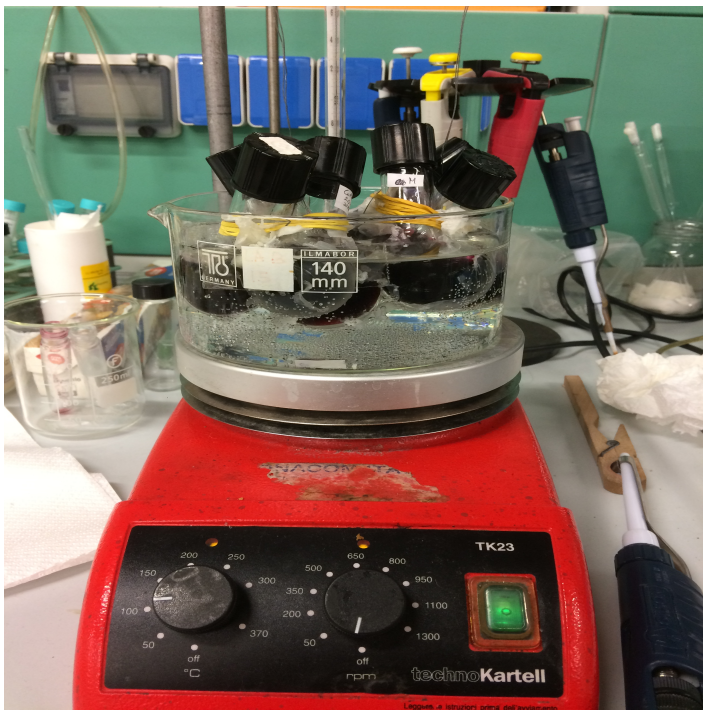

Figure 6 - Setup for the synthesis of nanoparticles at 70°C under vigorous magnetic stirring.

The absorption spectra were recorded at different times during the synthesis spectrophotometrically, at the wavelength 400-900nm with 2 nm steps. However, these had no clear peaks or notable change at 580 nm, which is mentioned in literature to be the peak absorbance for copper nanoparticles (64, 65) were detected. This could be caused by the overpowering absorbance of the extract itself, that itself has a purplish-red colour, making it difficult to observe. It could, of course, also mean that a very small portion of the ions are reduced to metallic NPs, although the TEM images indicate that metallic NPs have been made in the synthesis (Figure 9, Figure 10, Figure 12, Figure 14 and Figure 16)

4.1.2 Second synthesis of silver nanoparticles at 70°C

In Figure 7 we see the difference in colour between the extracts with and without silver nitrate. The *myrtillus* extract has a stronger red-violet colour, while the *gaultherioides* extract has a more transparent colour. The *myrtillus* extract does not change its colour even at higher concentrations of silver nitrate; it becomes more transparent, but keeps its purple colour. This might be because the *myrtillus* extract has a much stronger colour than the *gaultherioides* extract. The silver gives a slight grey-black tint to the solutions, as is more apparent in the tubes with *gaultherioides* extract. There was no change in colour from the start of the synthesis till the end; however, a dark coating that was quite difficult to remove, could be seen in the tubes. This is probably one of the silver salts with low solubility in water, e.g. Ag_2S (66). Some liquid silver salts that are exposed to light could also cause the dark colour, e.g. silver halides (67, 68). These same salts might also be the reason we see the grey-black tint in the samples after addition of silver nitrate. Samples were stored in a refrigerator at around 5°C, until further testing.

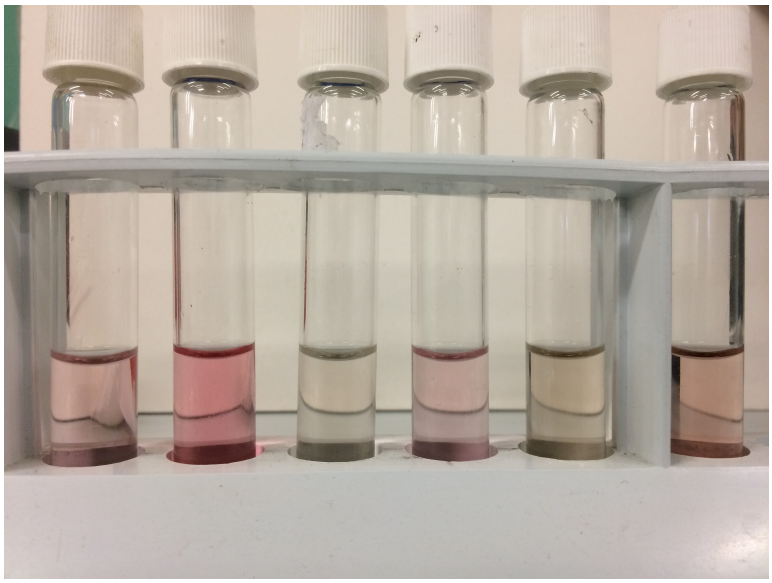

Figure 7 – Colour change of silver nanoparticles during the synthesis at 70°C. Diluted 1:39 (v/v) sample, makes it easier to see difference in colour. From left: *gaultherioides* (G) extract, *myrtillus* (M) extract, $AgNO_3$ 0.0125 M + G extract diluted 1:1 (v/v), $AgNO_3$ 0.0125 M + M extract diluted 1:1 (v/v), $AgNO_3$ 0.025 M + undiluted G extract, $AgNO_3$ 0.025 M + M.

4.2 Synthesis of copper and silver nanoparticles at 50°C

After addition of copper and silver metal precursor there was a slight colour change of the nanoparticle suspension. In tube 1 and 3 (see Table 6) were copper nitrate was added to extract, the suspension became slightly darker purple, while in tube 2 and 4 (see Table 6) were silver was added, the suspension got a greyish tint to them. The same colour was observed in tube 3 and 4 from the left in Figure 7, from the synthesis of silver nanoparticles at 70°C. There was no great change in colour from the start of the synthesis till the end of the synthesis. One might expect the colour of the suspensions with added copper solution to turn a bit more towards red; since $CuNO_3$ has a strong blue colour, while metallic copper nanoparticles should have a typical copper red colour (64). The next day, after they had been stored protected from light at room temperature (≈25°C), there was a purplish-black precipitate at the bottom of the tubes; this was easily re-suspended by shaking the tube. The samples were then stored in a refrigerator at around 5°C until further testing.

4.3 Purification of copper nanoparticles

After the first centrifugation (step 1 in purification process, section 3.6) there was a dark pellet at the bottom of the Eppendorf, while the liquid did not seem to have lost much of its original colour (see first and fifth tube in Figure 8). The pellet itself was very difficult to re-suspend, so a vortex was used to ease this process and save time. The suspension had a much lighter colour than the original suspension (second and sixth tube in Figure 8), the change was most detectable for the suspensions with the *gaultherioides* extract (tube 6). After the second re-suspension of the pellet, almost all colour disappeared from the suspension and after the re-suspension and centrifugation in MilliQ the liquid was colourless with just a weak tint of pink and the pellet was almost non-existent.

Figure 8 - Liquid decanted after each centrifugation step. From left to right: the 4 first tubes are $CuCl_2$ + *myrtillus*; First decanting, second decanting (with citric acid sol.), third decanting (with citric acid sol.), fourth decanting with MilliQ water. The 3 next tubes are $CuCl_2$ + *gaultherioides*. First decanting, second decanting (citric acid sol.), third decanting (with citric acid sol.).

Since almost all the extract seems to be lost during the purification process, there is not enough extract left to work as a capping agent for the nanoparticles. It also seems as though a great deal of the copper nanoparticles, and most certainly the ions, are lost during the process. A better way of preparing the nanoparticle suspension as well as a way of controlling particle size, would be to use a more diluted extract for the synthesis (22). Other groups that have washed/purified the copper nanoparticles used a much shorter purification procedure with only deionised water (22, 69). Citric acid was used to protect/reduce the amount of oxidation of the metallic Cu-NPs. The last washing with MilliQ water was to remove most of the citric acid, since it was thought it could work as a carbon source for the bacteria during the antibacterial testing. Suspensions containing citric acid would have been interesting to test, since the citric acid could have worked as a stabiliser for the nanoparticles, together with the extract (64, 70, 71).

4.4 Transmission electron microscopy

To determine if the synthesis of metal nanoparticles was successful, and to determine the particle size, the transmission electron microscopy was used. The metallic nanoparticles would be seen as dark spherical particles, in contrast to the crystalline structure of the precursor salts of the metals (10, 13, 22, 26, 33). As detectable in the TEM images after the purification of the copper nanoparticles (Figure 17-Figure 23), we can also see what is most likely copper oxide as the crystalline structures were also observed. This is to be expected since, as mentioned in the Introduction (section 1.1.3), the metallic copper will oxidise rather easily.

4.4.1 TEM images of nanoparticle suspensions of $CuCl_2$ + M/G and $Cu(Ac)_2$ + M/G synthesised at 70°C

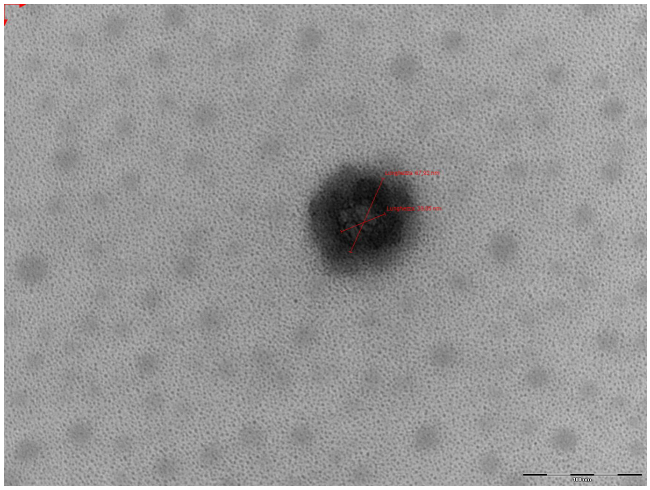

Figure 9 – $CuCl_2$ + *gaultherioides*.

Some larger aggregations around 50-100 nm in size were observed. Bar scale 100 nm.

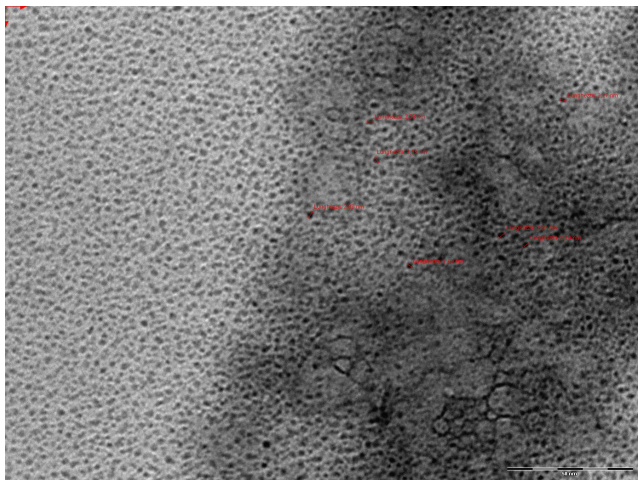

Figure 10 – $CuCl_2$ + *gaultherioides*.

Most of the sample consisted of very small spherical particles ranging from 2-4 nm. Bar scale 50 nm.

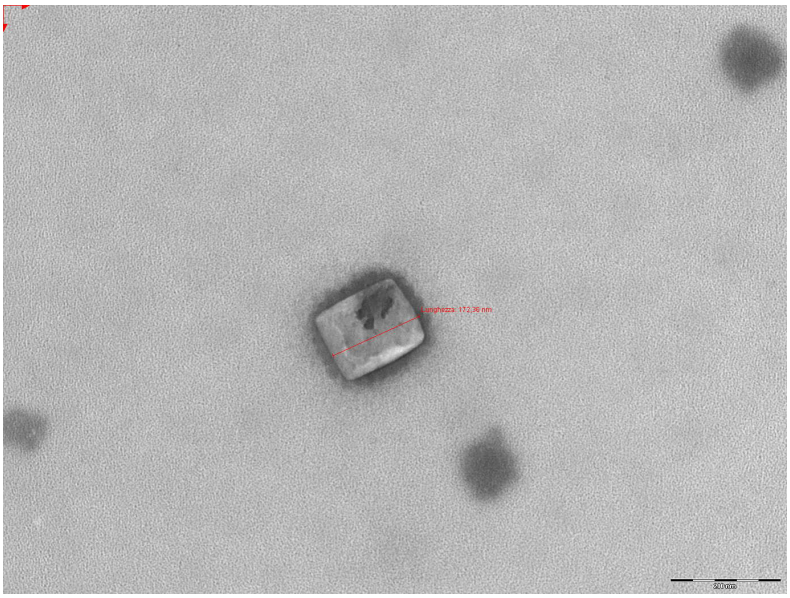

Figure 11 – $CuCl_2$ + *myrtillus*.

Several of these crystalline structures were observed, sizes ranging from 40-200 nm, with what seems to be aggregations of spherical particles and/or berry extract surrounding them. Bar scale 200 nm.

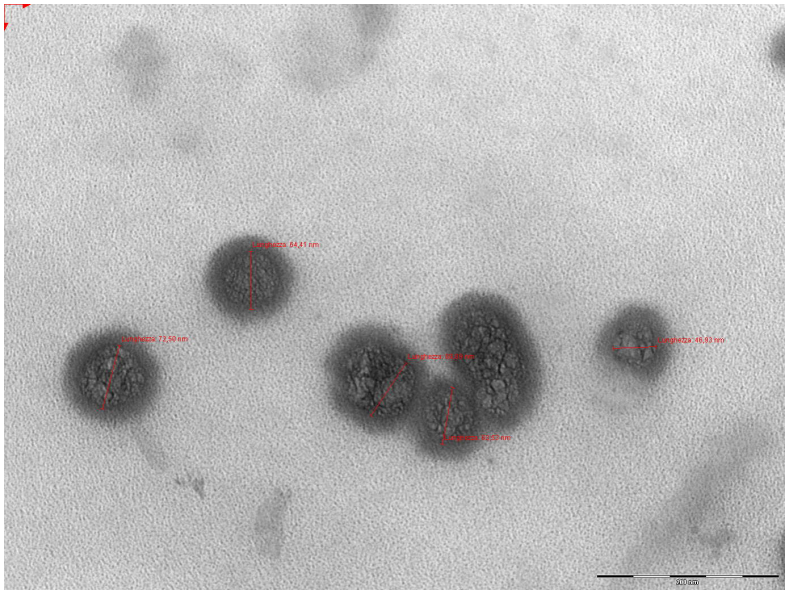

Figure 12 – $CuCl_2$ + *myrtillus*.

Spherical structures ranging from around 50-100 nm. Bar scale 200 nm.

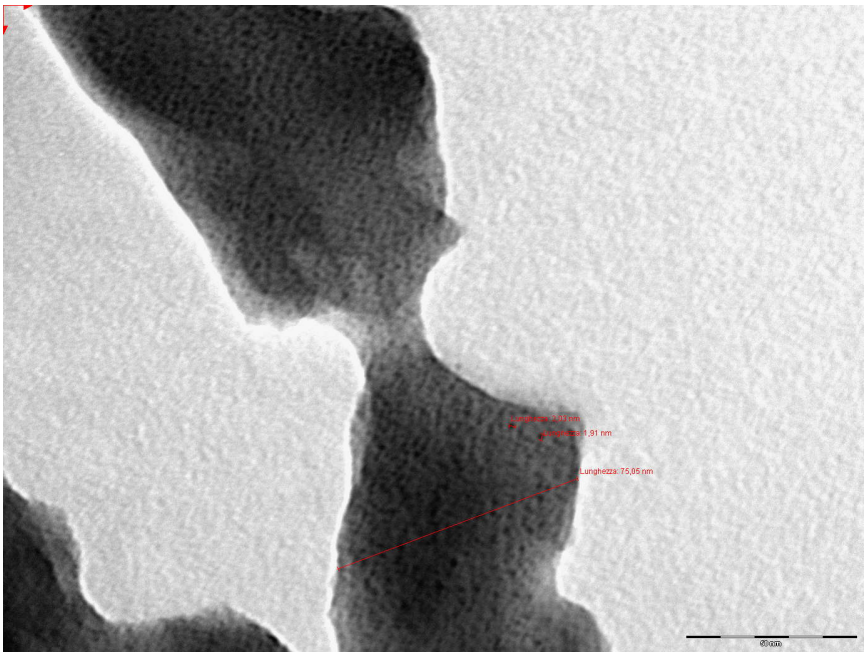

Figure 13 - $Cu(Ac)_2$ + *gaultherioides*.

A large amount of small spherical particles, trapped in a web of what is most likely the berry extracts. Bar scale 50 nm.

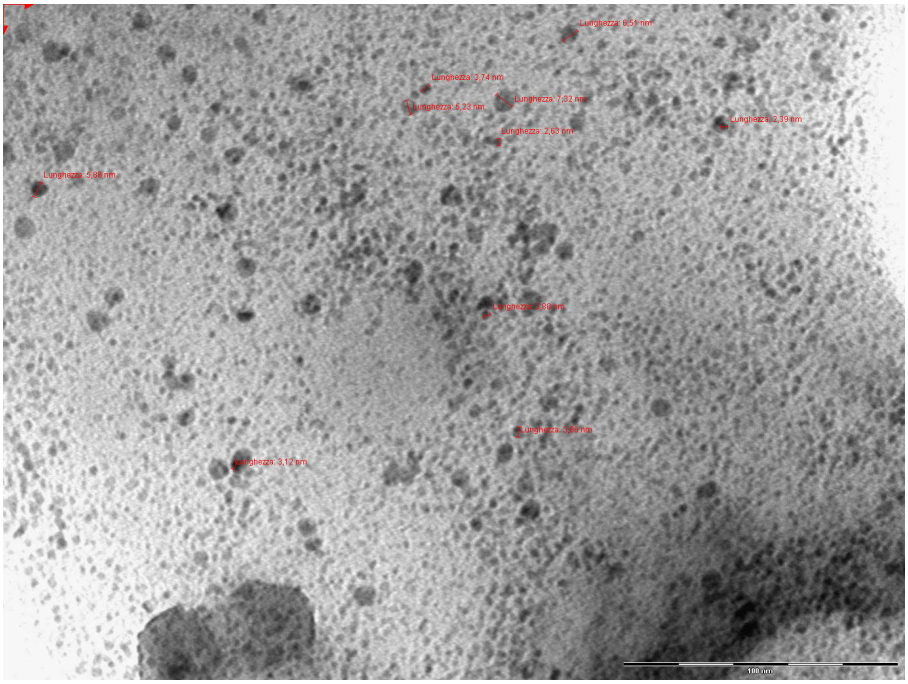

Figure 14 - $Cu(Ac)_2$ + *gaultherioides*.

Very small spherical particles ranging from around 3-10 nm. Bar scale 100 nm.

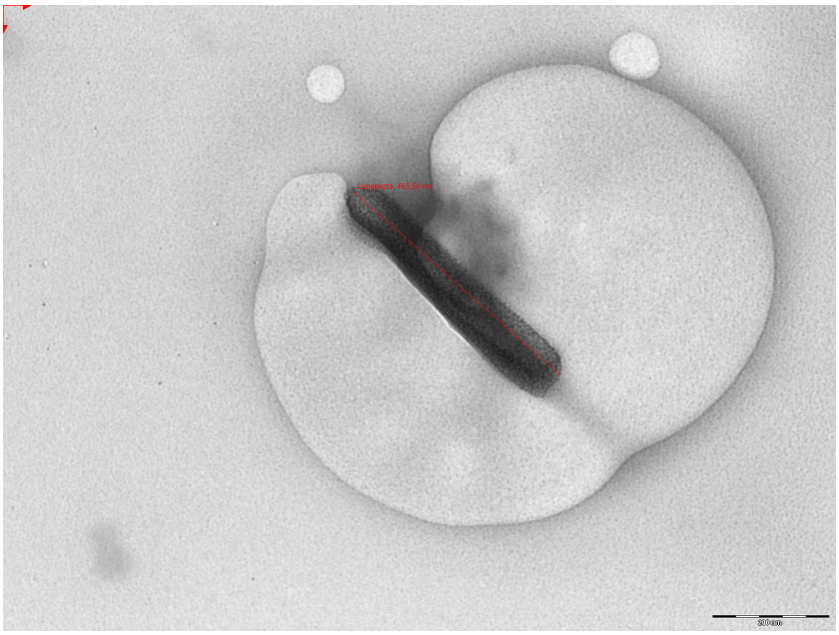

Figure 15 - $Cu(Ac)_2$ + *myrtillus*.

Several large rod-like structures were observed. Bar scale 200 nm

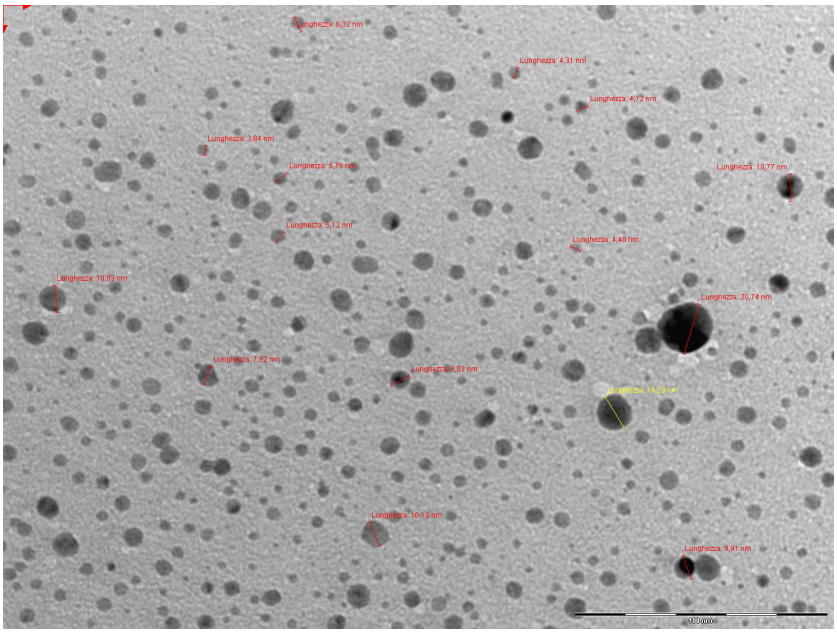

Figure 16 - $Cu(Ac)_2$ + *myrtillus*.

Large amounts of small spherical particles around 4-10 nm, a few larger particles above 20 nm were observed. Bar scale 100 nm.

4.4.2 TEM images of purified nanoparticle suspensions of $CuCl_2$ + M/G and $Cu(Ac)_2$ + M/G synthesised at 70°C

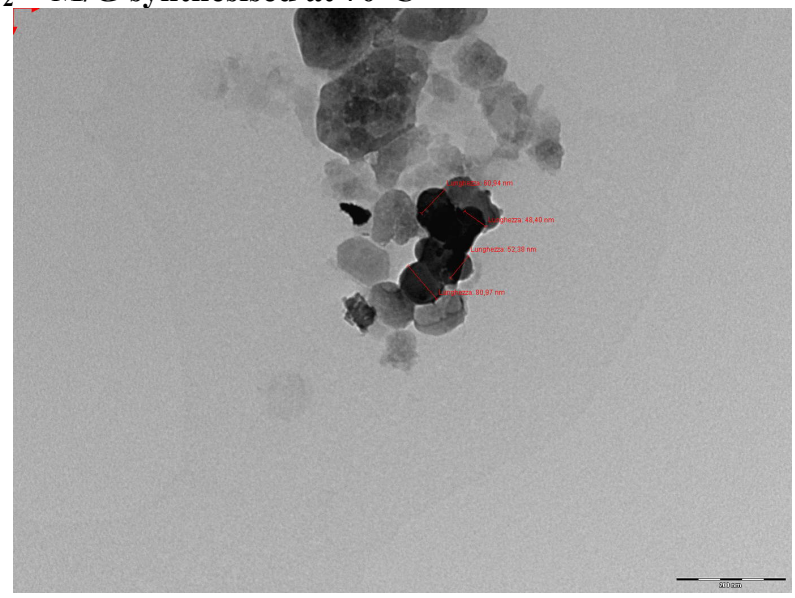

Figure 17 – Purified sample of $Cu(Ac)_2$ + *gaultherioides*.

Most of the sample contained crystallised structures in clusters like this. Ranging from small (around 10nm) to large 40-70 nm. Bar scale 200 nm.

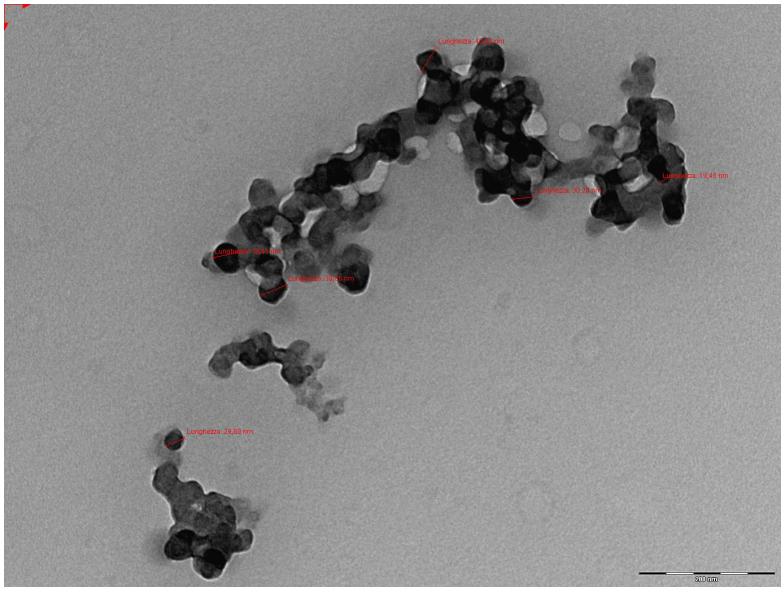

Figure 18 – Purfied sample of $Cu(Ac)_2$ + *gaultherioides*.

Clusters that might contain metallic nanoparticles. Bar scale 200 nm.

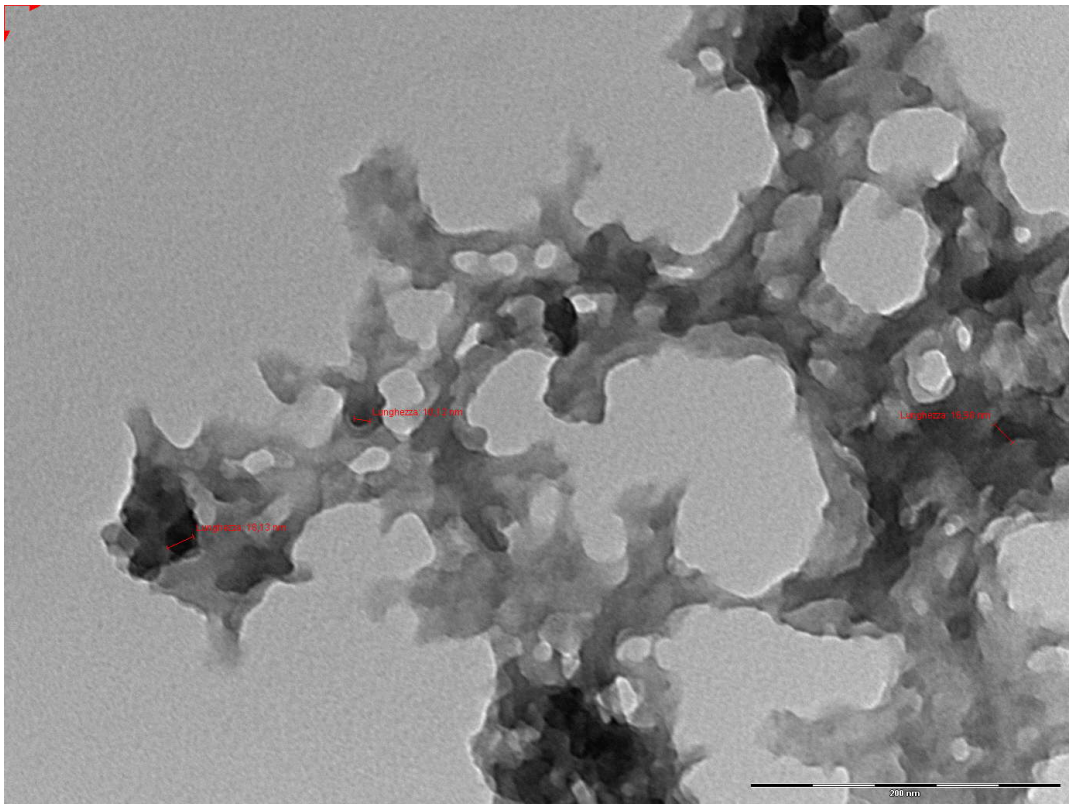

Figure 19 – Purified sample of $Cu(Ac)_2$ + *myrtillus*.

Sample contained mostly a mesh of the extract. Some particles were found, with a size ranging from 10-20 nm. Bar Scale 200 nm.

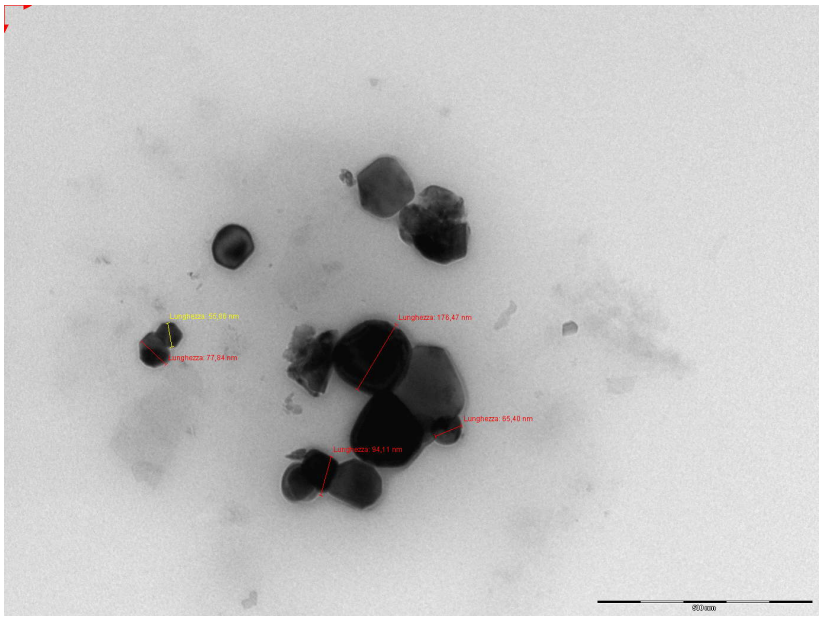

Figure 20 – Purified sample of $CuCl_2$ + *gaultherioides*.

Consisted of large crystallic particles, mostly in clusters. Bar scale 500 nm.

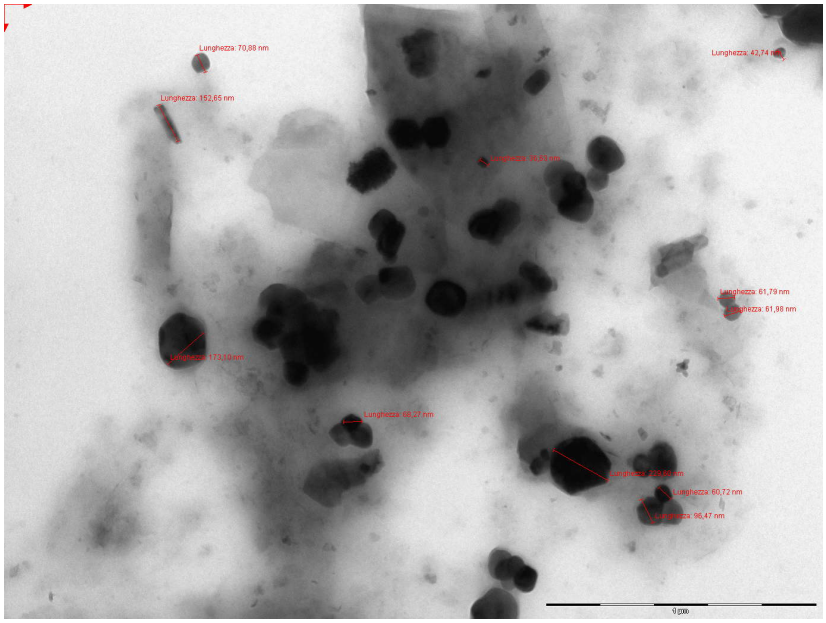

Figure 21 – Purified sample of $CuCl_2$ + *gaultherioides*.

Mostly crystallic particles with very different sizes and some rod structures. Bar scale 1 µm.

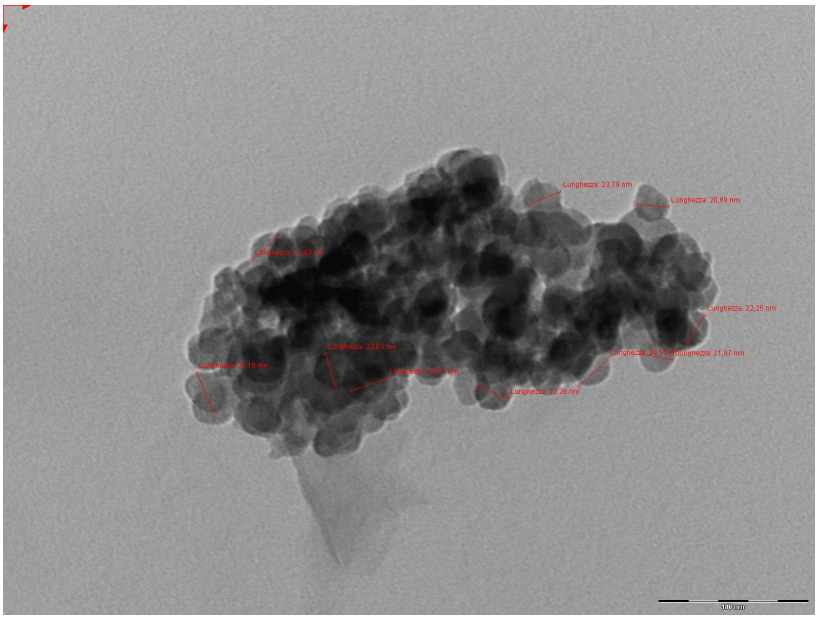

Figure 22 – Purified sample of $CuCl_2$ + *myrtillus*.

Large tight clusters with particles ranging from 20-25 nm. Bar scale 100 nm.

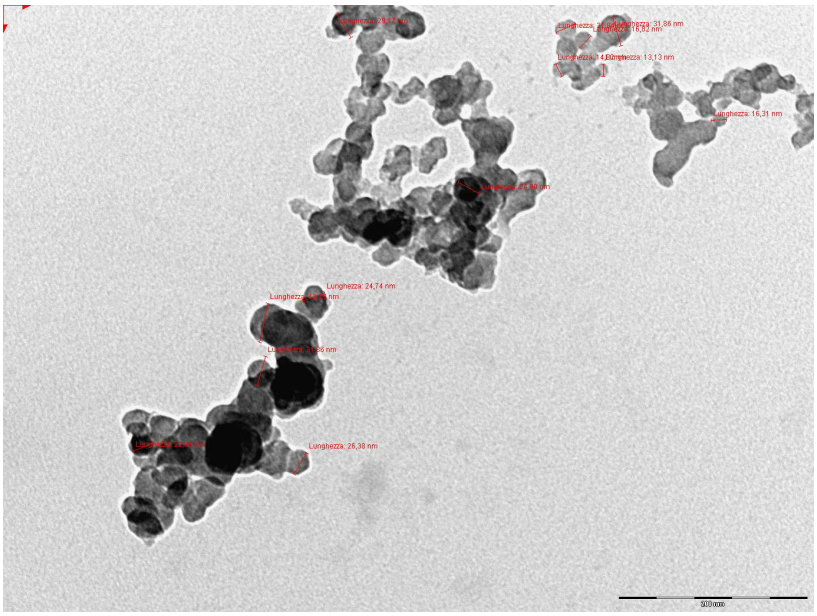

Figure 23 – Purified sample of $CuCl_2$ + *myrtillus*.

More clusters that also shows the mix of what seems to be the metallic nanoparticles and crystalline structures. Size from around 10 nm to 30 nm. Bar scale 200 nm.

4.4.3 TEM images of nanoparticle suspensions of $AgNO_3$ and $CuNO_3$ (0.0125M) nanoparticles + M/G (diluted 1:1, v/v) synthesised at 50°C

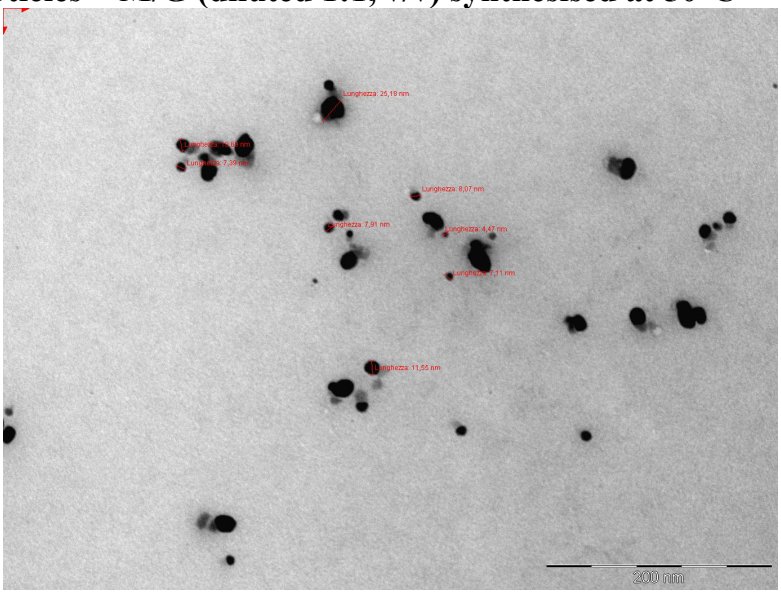

Figure 24 – $AgNO_3$ + *myrtillus*.

The sample has a wide distribution of size, mostly spherical particles from 7-15 nm. A few particles were quite a bit larger, ranging from 20-30 nm. Bar scale 200 nm.

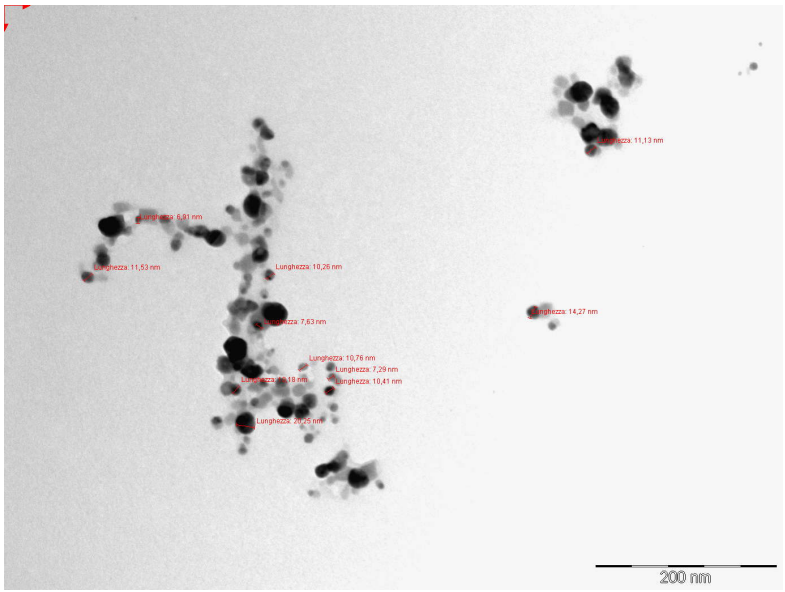

Figure 25 – $AgNO_3$ + *gaultherioides*.

Sample contains mostly spherical particles ranging from around 7-11 nm. A few larger particles around 20 nm were also observed. Bar scale 200 nm.

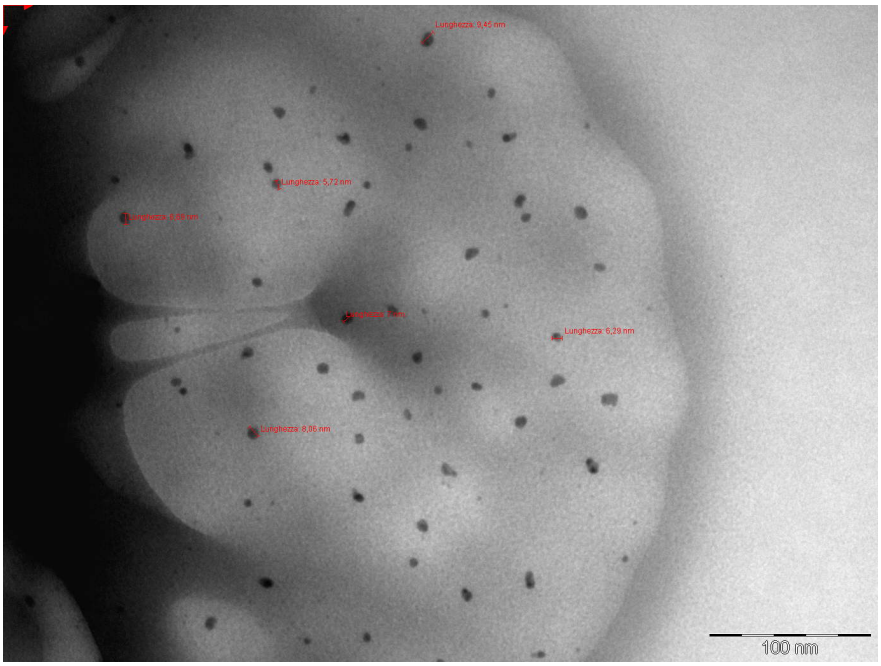

Figure 26 – $CuNO_3$ + *myrtillus*.

A large part of the sample consists of spherical nanoparticles around 6 nm. Bar scale 100 nm.

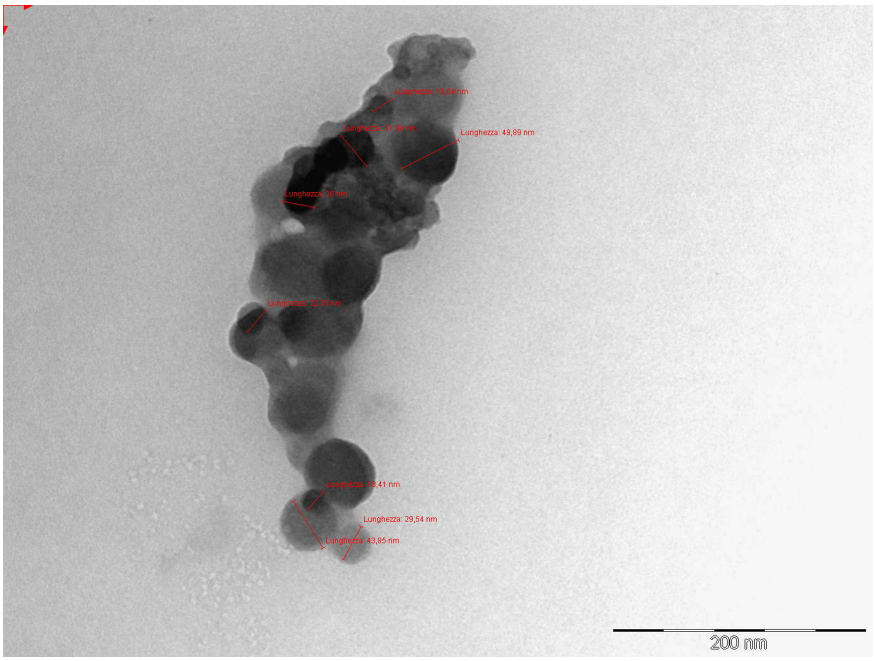

Figure 27 – $CuNO_3$ + *myrtillus*.

Some aggregates of nanoparticles, ranging from 20-50 nm, much larger than rest of the sample were found. Bar scale 200 nm.

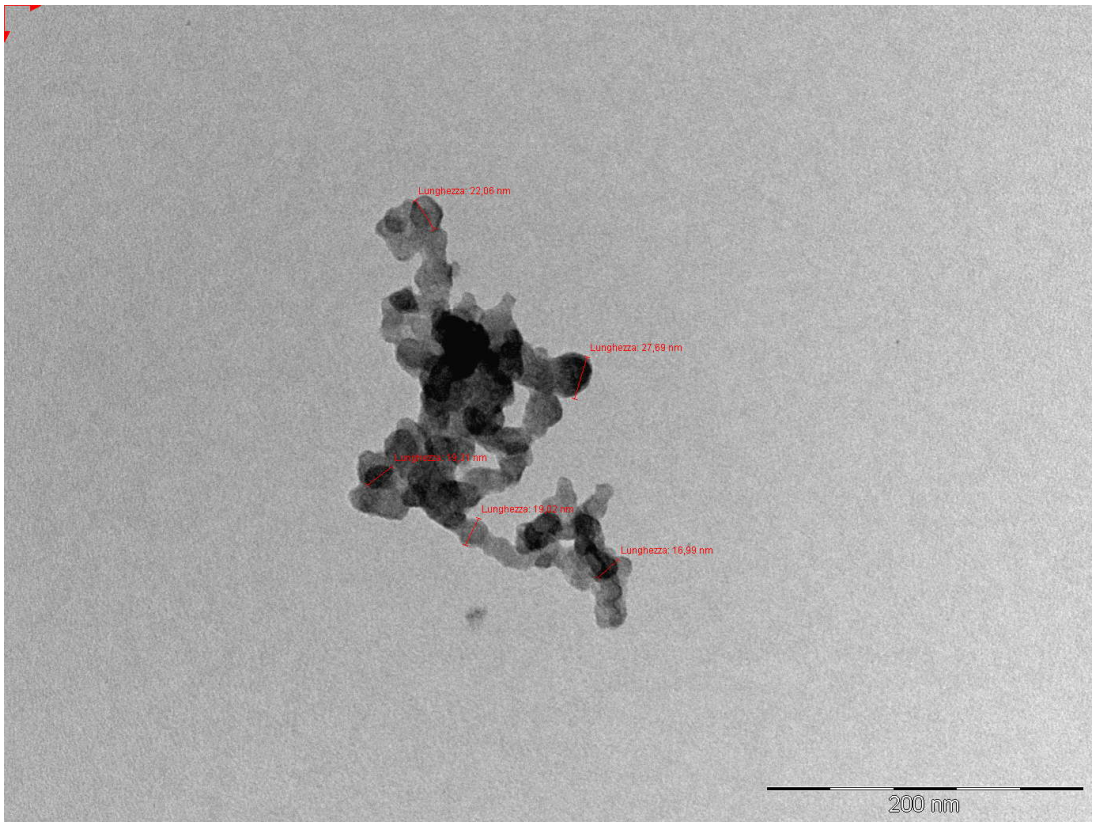

Figure 28 – $CuNO_3$ + *gaultherioides*.

Sample consisted of aggregates of nanoparticles with sizes ranging from 17-30 nm. Bar scale 200 nm.

4.4.4 TEM images of nanoparticle suspensions of $AgNO_3$ at 0.025M with undiluted extract and $AgNO_3$ at 0.0125M with extract diluted 1:1. Synthesised at 70°C

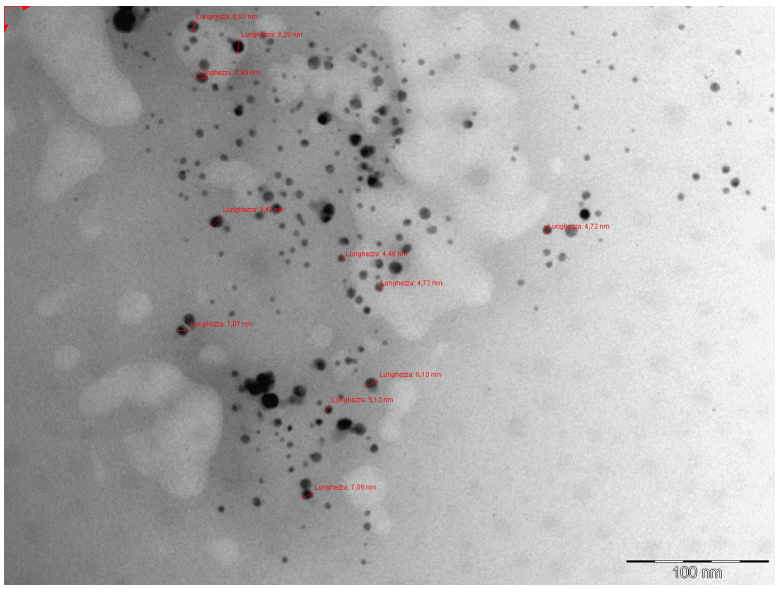

Figure 29 - AgNO (0.025) + undiluted *gaultherioides* extract.

Small spherical nanoparticles ranging from 5-10 nm was observed. Bar scale 100 nm.

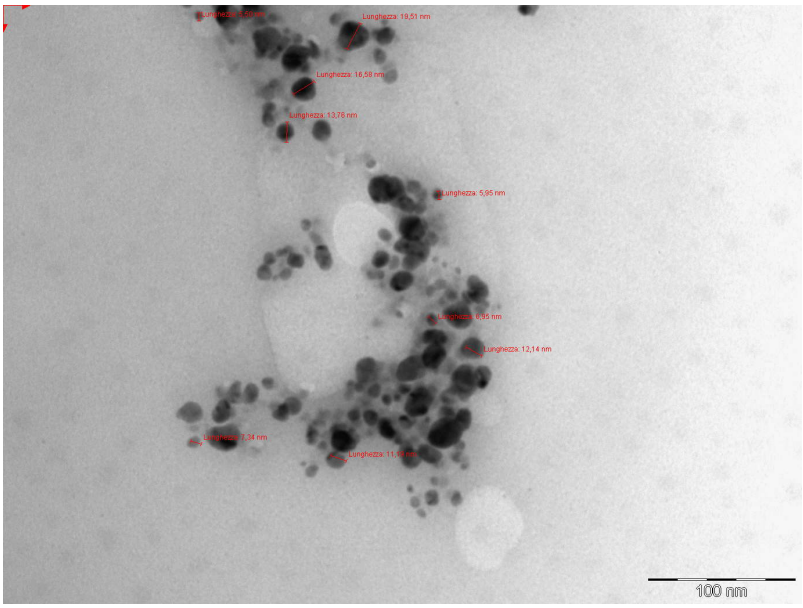

Figure 30 - AgNO (0.025) + undiluted *gaultherioides* extract.

Some loose aggregations of small spherical nanoparticles 5-20 nm. Bar scale 100 nm.

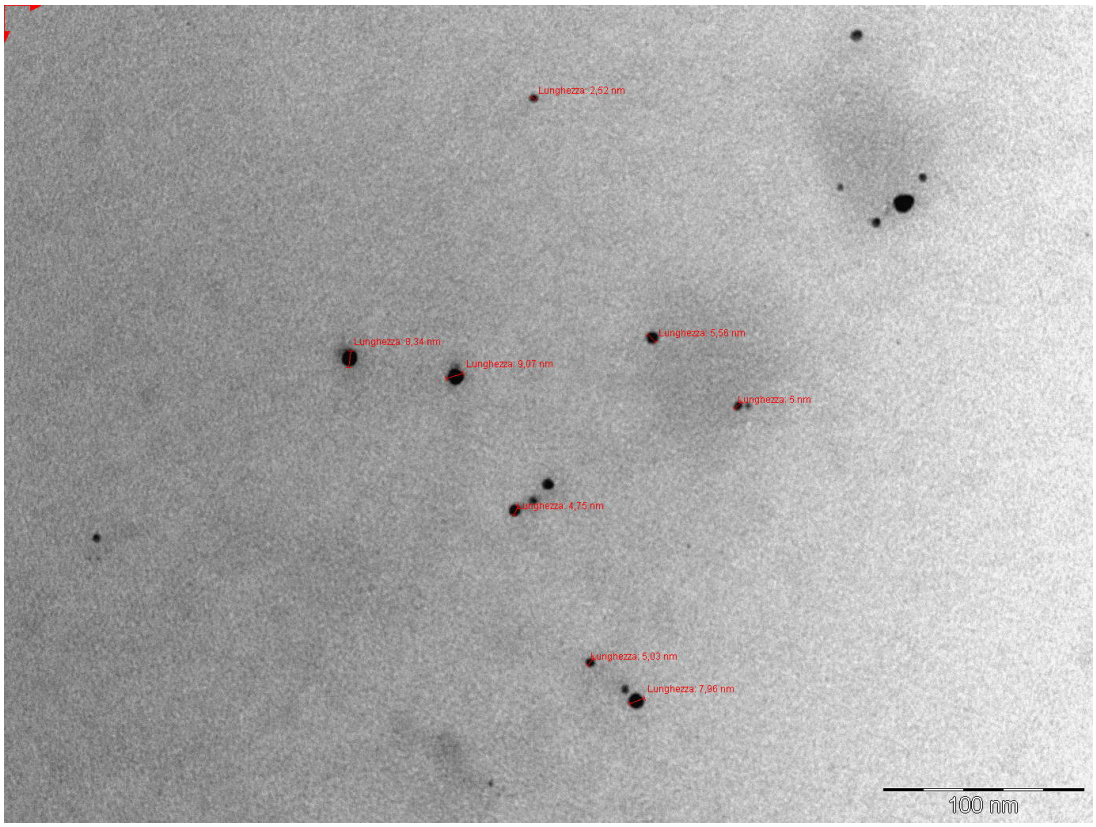

Figure 31 – $AgNO_3$ (0.0125) + *gaultherioides* extract diluted 1:1 (v/v).

A sparse amount of nanoparticles ranging from 5-10 nm was observed. Most of the particles were around 5 nm. Bar scale 100 nm.

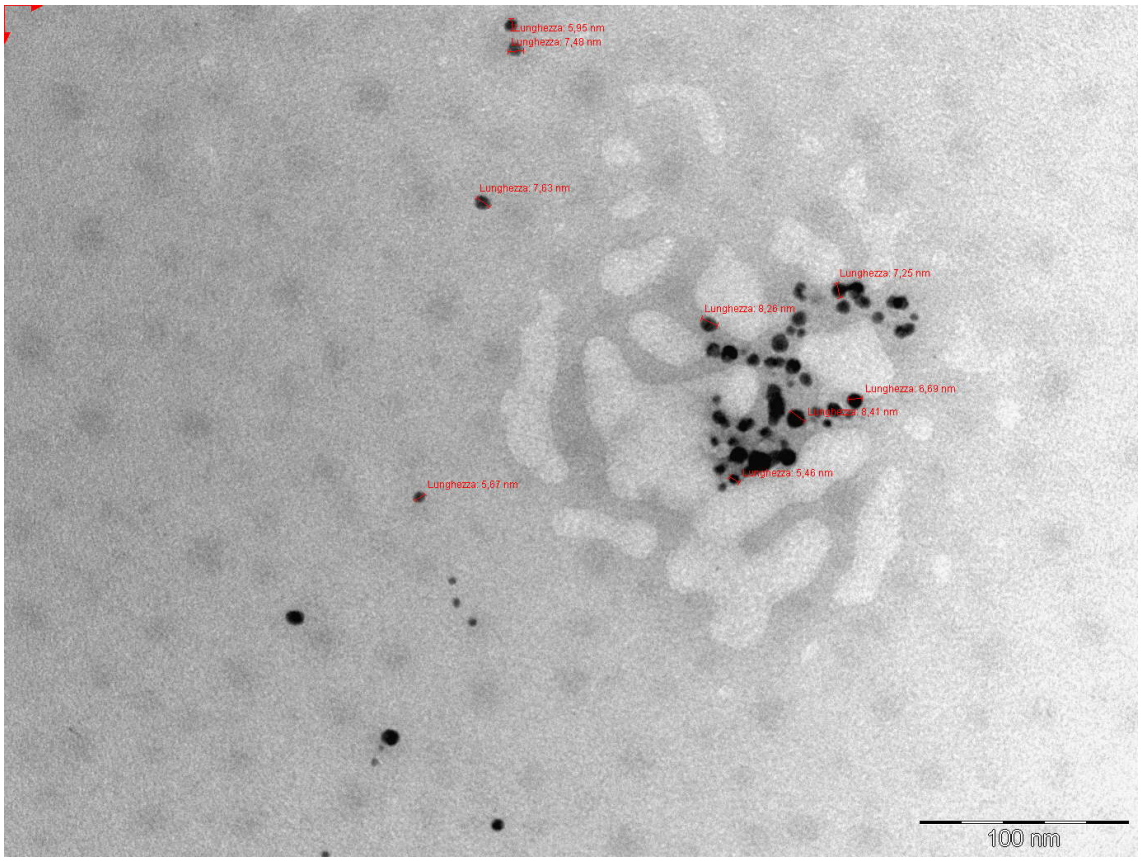

Figure 32 - $AgNO_3$ (0.025) + undiluted *myrtillus* extract.

Mostly loose aggregates of spherical nanoparticles ranging from 6-10 nm.

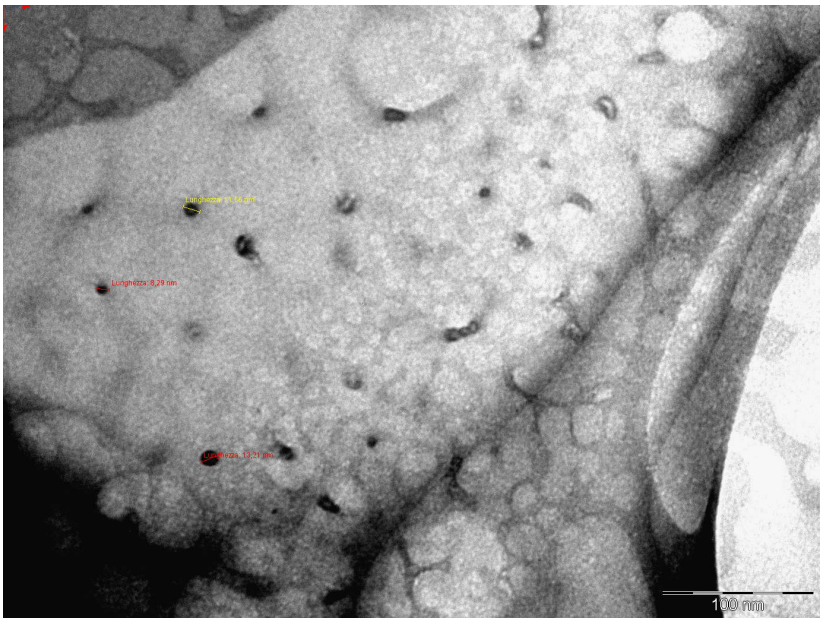

Figure 33 – $AgNO_3$ (0.0125M) + *myrtillus* extract diluted 1:1 (v/v).

A sparse amount of free spherical nanoparticles around 8-14 nm was observed. Bar scale 100 nm.

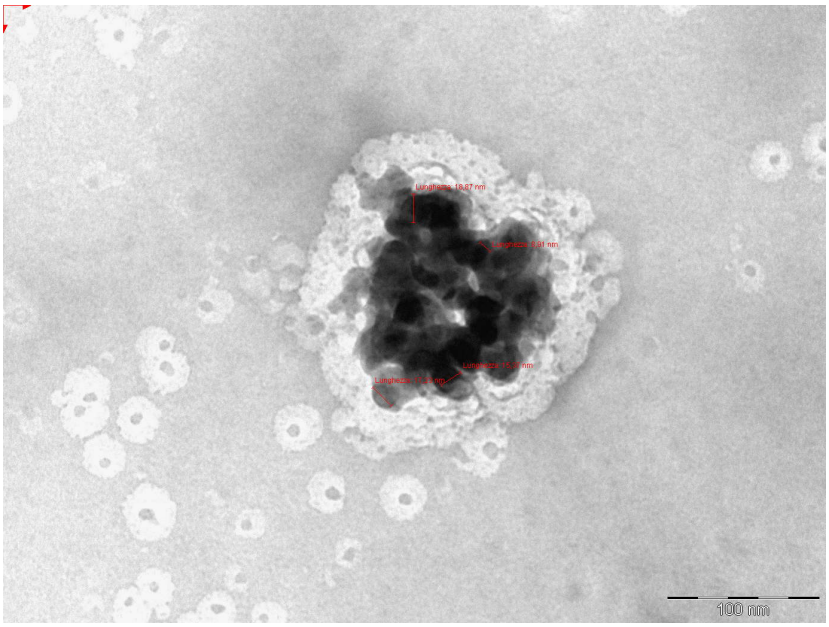

Figure 34 – $AgNO_3$ (0.0125M) + diluted *myrtillus* extract 1:1 (v/v).

Several aggregations of this size were seen in the sample. The spheres varied in sizes from around 10 nm to more than 100 nm. Bar scale 100 nm.

The descriptive summary of the observed TEM images is presented in Table 8.

Table 8 - Summary of nanoparticle sizes as determined in TEM analysis

Synthesis at 70°C with forceful magnetic stirring	**Sizes determined in TEM**	**Synthesis at 50°C with an orbital shaker**	**Sizes determined in TEM**
$CuCl_2$ 0.025 M + *myrtillus*	Few spherical particles 50-100 nm	$CuNO_3$ 0.0125M + *myrtillus*	6-10 nm
$Cu(Ac)_2$ 0.025 M + *myrtillus*	4-10 nm	$CuNO_3$ 0.0125M + *gaultherioides*	15-30 nm
$CuCl_2$ 0.025 M + *gaultherioides*	5-10 nm	$AgNO_3$ 0.0125M + *myrtillus*	5-20 nm
$Cu(Ac)_2$ 0.025 M + *gaultherioides*	3-10 nm	$AgNO_3$ 0.0125M + *gaultherioides*	5-20 nm
$AgNO_3$ 0.0125 M + *myrtillus*	8-18 nm		
$AgNO_3$ 0.0125 M + *gaultherioides*	5-8 nm		
$AgNO_3$ 0.025 M + *myrtillus*	4-9 nm		
$AgNO_3$ 0.025 M + *gaultherioides*	5-10 nm		

TEM images from the first synthesis with the *gaultherioides* extract show very small, spherical nanoparticles ranging 3-10 nm (Figure 10, Figure 13 and Figure 14), with some large particles of 50-100 nm in the sample with $CuCl_2$ + *gaultherioides* extract (Figure 9). The samples with *myrtillus* extract had a higher number of larger particles. $CuCl_2$ + M showed several large, crystalline structures (Figure 11), possible salt crystals of unreacted precursor, and some spherical nanoparticles ranging from 50-100 nm (Figure 12). The samples that had $Cu(Ac)_2$ as a metal precursor had several rod-shaped particles (Figure 15), but also a large amount of small spherical nanoparticles ranging from 4-10 nm (Figure 16). The nanoparticles, with the same concentration of metal precursor and extract, synthesised at 70°C are smaller than those synthesised at 50°C. This to be expected considering other reports on similar findings (22). No attempts to synthesise nanoparticles at a higher temperature than 70°C were done since the polyphenols might decompose, lowering the reducing capabilities of the extract. Prior to the synthesis at elevated temperature, one should evaluate the stability of extracts. This is also the reason that the extract and nanoparticle suspension was protected from light as much as possible; UV-light exposure decomposes polyphenols as well (72-74). Also since this was an attempt of a green chemistry approach to the synthesis of metal nanoparticles, lower temperatures were preferred because of the energy saving aspect. The synthesis of metal nanoparticles at room temperature (≈ 25°C) was not performed, since it would most likely be a much slower process (22) and the synthesis would not have a defined "end". This might cause very different results according to what time the metal precursor and extract was mixed, and at what time the tests were performed.

As seen in the TEM images of the purified samples (Figure 17-Figure 23), there is a large degree of crystallisation, meaning there is little or no metallic copper (Cu^0) nanoparticles left in the suspension. Which is to be expected considering how easily metallic copper is oxidised (see introduction section 1.1.3). Since a large amount of the capping agents are removed during the purification procedure, the surface of the nanoparticles are less resistant to

oxidation . Therefore, it was decided not to perform a purification of the nanoparticles made in later synthesises.

It was hypothesised that the lack of antibacterial effect from the copper nanoparticles might be because the particles were too small, since most studies use Cu-NPs that are quite larger than what we have prepared here; around 20 nm or larger (22, 23, 44). One study prepared Cu-NPs that were around 5-10 nm that showed antibacterial effect and non-cytotoxicity (75). However, this might be because their NPs were considerably more stable and they did not have the same problems regarding aggregation and precipitation.

A new synthesis was therefore performed using an orbital shaker, lower temperature and lower concentration of both metal precursor and extract. From the TEM images of the samples from this synthesis we see that the nanoparticles are in general larger (Figure 24-Figure 28) than the nanoparticles prepared at a higher temperature and with more vigorous stirring (Figure 9-Figure 16 and Figure 29-Figure 34). Another way to control size could be by adjusting the amount of metal precursor but keeping extract undiluted, or by keeping metal precursor concentration the same and diluting the extract. This has been done by others as a way of modifying size of copper and silver nanoparticles (22, 46).

4.5 X-ray photoelectron spectroscopy

The XPS analysis showed no signs of copper, copper oxide or any of the copper salt precursors, neither for the purified or untreated samples. Considering the high loss of both extract and most likely Cu-NPs and copper ions, after the purification process, it could be expected not to detect them in the XPS analysis. Since the XPS is only able to read the surface area of the sample (ca. 0-10 nm), the reason that we could not detect the copper in the untreated samples might be because of the amount of extract that is now covering the Cu-NPs and the unreacted metal precursor salt. Others did not encounter the same problem, although they used a diluted extract for their synthesis than we did (22).

4.6 Antimicrobial potential of nanoparticles

The exact concentration of metal nanoparticles in the suspensions is not determined, but we know that metal nanoparticles should exhibit a greater antibacterial effect than the salt solution. Therefore, one would expect more inhibition of bacteria by samples containing nanoparticles than for the salt solutions. The aggregation and precipitation observed during storage of the nanoparticles may interfere with the testing, especially those where the suspensions are static (broth microdilution on microtiter plates and agar disk diffusion tests).

4.6.1 Agar diffusion testing

After incubation at 37°C the diameter of the inhibition zone was measured. Results are summarised in Table 9 below.

Table 9 – Inhibition zone (mm) for samples from the first synthesis.
* = No growth observed underneath the disks. 1 parallel for each strain.

#	Sample	*E. coli* ATCC 35218	*S. aureus* ATCC 25923	*S. aureus* ATCC 29213
1	M	-	-	-
2	G	-	-	-
-	Ampicillin (1 µg/mL)	-	30	21
-	NaCl 0.9%	-	-	-
3	$CuCl_2$ 0.025M	8.0	-	*
4	$Cu(Ac)_2$ 0.025M	-	-	*
5	$CuCl_2$ + M	6.5-7.0	-	6.5
6	$Cu(Ac)_2$ + M	-	6.5	7.0
7	$CuCl_2$ + G	-	-	7.5
8	$Cu(Ac)_2$ + G	-	-	-
9	Purified $CuCl_2$ + M	-	-	-
10	Purified $Cu(Ac)_2$ + M	-	-	-
11	Purified $CuCl_2$ + G	-	-	-
12	Purified $Cu(Ac)_2$ + G	-	-	-
13	Purified, 2x concentration $CuCl_2$ + M	-	-	-
14	Purified, 2x concentration $Cu(Ac)_2$ + M	-	-	-
15	Purified, 2x concentration $CuCl_2$ + G	-	-	-
16	Purified, 2x concentration $Cu(Ac)_2$ + G	-	-	-

As seen in Table 9 the *S. aureus* ATCC 29213 seems to be more sensitive to the copper, both the ions and the nanoparticle samples. None of the purified samples exhibited any antibacterial effect, which might be because a large amount of the copper is lost in the purification process.

Additionally, as seen in the TEM images of the purified samples (Figure 17-Figure 23), there might be only copper oxide left, and no metallic copper nanoparticles. As seen in for the copper salt solution controls (Number 3 and 4 in Table 9) against *S. aureus* ATCC 29213, there was no growth of *S. aureus* directly underneath the disk, but no inhibition beyond the disk. This made us suspect that the agar absorbs too much of the metal ions and nanoparticles, and not letting them diffuse properly. Therefore, it was decided not to use the disk diffusion test for testing the antibacterial effect of the nanoparticles from the other synthesises.

Other studies using disk diffusion testing did not report the same problem (45, 65). Since one could also see aggregation and precipitation of what is most likely metal nanoparticles and some extract when the suspensions are left standing for a couple of hours, it was decided not to use the disk diffusion test for antibacterial testing of the samples from the other synthesises. Another reported method used for testing of the copper nanoparticles consisted of a sterile latex sponge dipped in copper nanoparticle solution and then put in a flask of liquid medium (22), however, these materials and amount of copper nanoparticles were not available. It was decided that a liquid medium antibacterial testing might be a better way of testing the antibacterial activity.

4.7 Antibacterial testing in tubes with liquid medium

Only the *S. aureus* ATCC 29213 strain was used in the antibacterial testing in tubes with liquid medium, since it showed more sensitivity to the copper nanoparticles. Our version of the test is very similar to the one used by Lee et al (22), but instead of using a sponge dip-soaked in the nanoparticle suspension we put the suspension directly into the tube. In Table 10 the results of the counting of the bacterial colonies after plating of the tubes incubated in an orbital shaker for 24 hours at 37°C at 130 rpm are summarized. The purified samples showed no inhibition of bacterial growth, which might be because a large loss of metal NPs during the purification process. It is worth noticing that it seems the extracts alone have some inhibiting effect on bacterial growth; this was not seen in either the disk diffusion test or the microtiter plate test. The non-purified nanoparticle suspensions (#5-8 in Table 10) seem to affect the growth of bacteria, however the plates appear to be contaminated (Figure 35).

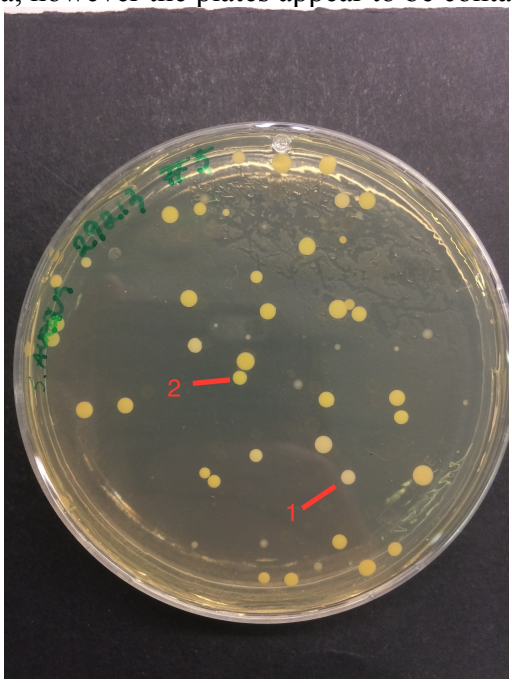

Figure 35 - Plate of sample #5 (see Table 10) $CuCl_2$ + *myrtillus* extract. 1 = colony with a very strong yellow colour not similar to the *S. aureus* strain that was inoculated in the liquid medium. 2 = White colony that is slightly off compared to the white coloured colonies of the *S. aureus* strain that was inoculated.

The reason that this test gave result different from the disk diffusion test is most likely because the extract and nanoparticles tended to aggregate and sediment. Since the disk diffusion and microtiter plates are static, all the particles stay in one place or sediment, making it difficult for the nanoparticles to affect the bacteria. Lee et al. (22) found that their biologically synthesised Cu-NPs were stable for up at least 30 days, compared to their chemical synthesis of Cu-NPs which precipitated within 24 hours. They also saw that the more stable Cu-NPs exhibited stronger antibacterial effect than the less stable Cu-NPs. Keeping the Cu-NPs suspended during the incubation might be one of the reasons we see more growth inhibition than in the other two antibacterial tests. What should also be noted is that since the medium is water based and the tubes are agitated, there is an increased risk that a large amount of the metallic Cu-NPs have been oxidised. This is not necessarily all negative, since CuO also has been shown to show antibacterial effect (63, 76), but it makes it difficult to evaluate the antibacterial effect of the metallic Cu-NPs alone. It might also be that

it was simply too low concentration of Cu-NPs, CuO and copper ions to exhibit an antibacterial effect, therefore higher concentrations should be tested. It could also be that the concentration of the extract is too high, covering the copper and restricting it from exerting its effect on the bacteria. Clearly, it is crucial to optimize the concentration of extracts used in the green synthesis.

It would have been interesting to try a liquid medium antibacterial test on an *E. coli* or *B. subtilis* strain too, since antibacterial effect has been detected against both of these bacteria in other studies; even greater activity than Ag-NPs against *B. subtilis* was reported (22, 44, 45).

Table 10 – Antimicrobial evaluation. 1 parallel with *S. aureus* ATCC 29213.
*= Contamination because none of the colonies resemble the colour or shape of inoculated *S. aureus* strain.

#	Sample	Result
1	M	3 visible colonies
2	G	No growth
3	$CuCl_2$ 0.025M	No growth
4	$Cu(Ac)_2$ 0.025M	11 colonies, most likely contamination*
5	$CuCl_2$ + M	51 colonies, most likely contamination*
6	$Cu(Ac)_2$ + M	5 colonies, most likely contamination*
7	$CuCl_2$ + G	80 colonies, at least 2 contaminants*
8	$Cu(Ac)_2$ + G	8 colonies, most likely contamination*
9	Purified $CuCl_2$ + M	No inhibition
10	Purified $Cu(Ac)_2$ + M	
11	Purified $CuCl_2$ + G	
12	Purified $Cu(Ac)_2$ + G	
13	Purified, 2x concentration $CuCl_2$ + M	
14	Purified, 2x concentration $Cu(Ac)_2$ + M	
15	Purified, 2x concentration $CuCl_2$ + G	
16	Purfied, 2x concentration $Cu(Ac)_2$ + G	

4.8 Sensitivity assays

Exact concentration of the metal nanoparticles is not known, since there was no way of measuring it. The synthesis will most likely not reduce 100% of the copper and silver ions to metallic copper and silver nanoparticles. Since the ions themselves should have some antibacterial effect we operated with the concentration to be more or less the same as for the concentration of metal precursor. If the metallic nanoparticles had greater antibacterial effect than the ions, as seen in several other studies (49, 50), we should have seen a decreased MIC for the samples compared to the copper and silver salt solutions.
The purified Cu-NP formulations did not show any antibacterial effect in both concentrations that were prepared. This, along with the TEM images showing a large grade of crystallisation, is why it was decided not to purify the nanoparticles from the other synthesises.
As seen in the tables in the Appendix there is a very high absorbance in the wells with the highest concentration of NPs. For example, as seen in Table 22 row D, the absorbance is very high in column 1-4, but in column 5 it reaches its lowest point before increasing again from column 6 and onwards. It would be reasonable to assume that the absorbance seen in the first wells is then caused by the colour of the sample, and as the concentration of sample decreases, the bacteria are no longer inhibited and starts growing again from the well in column 6. This could also mean that if the wells up to column 5 had been plated, we would have seen an inhibition of growth. In row F and H (Table 22) we see that for the Ag-NP suspensions the problem with disturbance of OD was smaller. The disturbance is much lower for the H row, were the extract has already been diluted. For the Ag-NP suspensions there was a much smaller pellet in these wells, also for the Ag-NPs synthesised at 70°C and for both concentrations 0.0125 M and 0.0250 M. This means that the Ag-NPs are probably more stable in suspension than the Cu-NPs.

It was observed that wells containing sample had a small pellet of dark material in the bottom, especially in the wells with higher concentration. This is most likely the same kind of precipitate as seen in the tubes when they are left standing for a while, and one of the reasons the disk diffusion test did not work properly. The interference of the extract on the absorbance makes it difficult to get a correct reading. A reading of the plate at t_0 (just after adding of the bacteria) should have been done. This way the difference in Optical Density (OD) could have been calculated: $\Delta OD = t_{24}-t_0$. If there had been time, the wells would have been plated to accurately define a MIC value. Others who used microtiter plates for testing metal nanoparticles, plated the wells to determine MIC, used a colour indicator or an automatic microtiter fluorescence assay (77-79). One could also have attempted to put the microtiter plates on a shaker during the incubation, which would help keep the nanoparticles dispersed in the suspension. Changing the synthesis to different metal concentrations and dilutions of the extract could make a composition that stays stable for longer, which in turn could have increased antibacterial effect compared to the suspensions prepared in these experiments (22, 27, 33).

4.9 Cytotoxicity assay

Although we have not detected the expected antimicrobial activity of NPs, it was important to evaluate their potential toxicity. Considering that silver NPs are widely used as wound dressings (40, 51), we selected one of the most commonly used keratinocytes as a model cells to determine potential cytotoxicity.

The results of the cytotoxic assay are presented below in simplified tables of the microplate readings (Table 11-Table 13).

Table 11 - Cytotoxicity results plate 1.

$CuCl_2$ and $Cu(Ac)_2$ ($2.5*10^{-2}$ M). CT = Cytotoxic, NCT = Live cells/not cytotoxic. * = Somewhat cytotoxic, interference of absorbance caused by colour of extract.

<table>
<tr><td></td><td></td><td></td><td colspan="3">1 µL sample</td><td colspan="3">5 µL sample</td><td colspan="3">10 µL sample</td><td></td><td></td></tr>
<tr><td></td><td></td><td>1</td><td>2</td><td>3</td><td>4</td><td>5</td><td>6</td><td>7</td><td>8</td><td>9</td><td>10</td><td>11</td><td>12</td></tr>
<tr><td></td><td>A</td><td colspan="12">Blank wells</td></tr>
<tr><td>G</td><td>B</td><td rowspan="3">Blank</td><td colspan="3">NCT</td><td colspan="2">NCT</td><td>CT</td><td colspan="3">NCT?*</td><td rowspan="3">Control</td><td rowspan="7">BLANK</td></tr>
<tr><td>M</td><td>C</td><td colspan="3">NCT</td><td colspan="3">CT</td><td colspan="3">CT</td></tr>
<tr><td>$Cu(Ac)_2$ + G</td><td>D</td><td colspan="3">CT</td><td colspan="3">CT</td><td colspan="3">CT</td></tr>
<tr><td>$Cu(Ac)_2$ + M</td><td>E</td><td rowspan="3">Control</td><td colspan="3" rowspan="3">CT</td><td colspan="3">CT</td><td colspan="3" rowspan="3">CT</td><td rowspan="3">Blank</td></tr>
<tr><td>$CuCl_2$ + G</td><td>F</td><td colspan="2">CT</td><td>NCT?</td></tr>
<tr><td>$CuCl_2$ + M</td><td>G</td><td colspan="3">CT</td></tr>
<tr><td></td><td>H</td><td colspan="12">Blank wells</td></tr>
</table>

Table 12 – Cytotoxicity results plate 2.

CuNO3 and AgNO3 (1.25*10-2 M). CT = Cytotoxic, NCT = Live cells/not cytotoxic. * = Somewhat cytotoxic, interference of absorbance caused by colour of extract.

<table>
<tr><td></td><td></td><td></td><td colspan="3">1 µL sample</td><td colspan="3">5 µL sample</td><td colspan="3">10 µL sample</td><td></td><td></td></tr>
<tr><td></td><td></td><td>1</td><td>2</td><td>3</td><td>4</td><td>5</td><td>6</td><td>7</td><td>8</td><td>9</td><td>10</td><td>11</td><td>12</td></tr>
<tr><td></td><td>A</td><td colspan="12">Blank wells</td></tr>
<tr><td>G</td><td>B</td><td rowspan="3">Blank</td><td colspan="3">NCT</td><td colspan="3">NCT</td><td colspan="3">NCT?*</td><td rowspan="3">Control</td><td rowspan="7">BLANK</td></tr>
<tr><td>M</td><td>C</td><td colspan="3">NCT</td><td colspan="3">NCT</td><td colspan="3">CT</td></tr>
<tr><td>$AgNO_3$ + G</td><td>D</td><td colspan="3">CT</td><td colspan="3">CT</td><td colspan="3">CT</td></tr>
<tr><td>$AgNO_3$ + M</td><td>E</td><td rowspan="3">Control</td><td colspan="3" rowspan="3">CT</td><td colspan="3" rowspan="3">CT</td><td colspan="3" rowspan="3">CT</td><td rowspan="3">Blank</td></tr>
<tr><td>$CuNO_3$ + G</td><td>F</td></tr>
<tr><td>$CuNO_3$ + M</td><td>G</td></tr>
<tr><td></td><td>H</td><td colspan="12">Blank wells</td></tr>
</table>

Table 13 - Cytotoxicity results plate 3.

$AgNO_3$ at concentrations of 0.0125 M and 0.025 M. CT = Cytotoxic, NCT = Live cells/not cytotoxic.
* = Somewhat cytotoxic, interference of absorbance caused by colour of extract.

<table>
<tr><td></td><td></td><td></td><td colspan="3">1 µL sample</td><td colspan="3">5 µL sample</td><td colspan="3">10 µL sample</td><td></td><td></td></tr>
<tr><td></td><td></td><td>1</td><td>2</td><td>3</td><td>4</td><td>5</td><td>6</td><td>7</td><td>8</td><td>9</td><td>10</td><td>11</td><td>12</td></tr>
<tr><td></td><td>A</td><td colspan="12">Blank wells</td></tr>
<tr><td>G</td><td>B</td><td rowspan="3">Blank</td><td colspan="3">NCT</td><td colspan="3">NCT*</td><td colspan="3">CT</td><td rowspan="3">Control</td><td rowspan="6">BLANK</td></tr>
<tr><td>M</td><td>C</td><td colspan="3">NCT</td><td colspan="3">NCT*</td><td colspan="3">CT</td></tr>
<tr><td>$AgNO_3$ (0.0125 M) + G</td><td>D</td><td colspan="3">CT</td><td colspan="3">CT</td><td colspan="3">CT</td></tr>
<tr><td>$AgNO_3$ (0.0125 M) + M</td><td>E</td><td rowspan="3">Control</td><td colspan="3">NCT?*</td><td colspan="3">NCT?*</td><td colspan="3">NCT?*</td><td rowspan="3">Blank</td></tr>
<tr><td>$AgNO_3$ (0.025 M) + G</td><td>F</td><td colspan="3" rowspan="2">CT</td><td colspan="3" rowspan="2">CT</td><td colspan="3" rowspan="2">CT</td></tr>
<tr><td>$AgNO_3$ (0.025 M) + M</td><td>G</td></tr>
<tr><td></td><td>H</td><td colspan="12">Blank wells</td></tr>
</table>

All suspensions containing metal nanoparticles tended to aggregate and precipitate; as a result all exhibited a high cytotoxic effect. The extract alone did not precipitate, which might explain why it does not show the same kind of cytotoxicity. At the higher concentrations of extract (the wells were 5 µL and 10 µL are added) we saw an increase in cytotoxicity. However, in the 5 µL wells for the extracts alone in plate 1 and 3 (Table 11 and Table 13) the OD was higher than in a well where there is no live cells left, but lower than in the control wells, which shows starting toxicity. The wells with 10 µL of the extract showed the same tendency. In those wells, as well as in all the wells with 10 µL of sample, the readings showed still higher absorbance than in the blank wells. This is probably because of the strong colour of the extract, which causes a higher reading of absorbance. The same was observed in the microtiter plates for antibacterial testing. To lower the toxicity, a way of stabilising the suspension should be developed. If the nanoparticles are kept in suspension, instead of aggregating and precipitating, the toxicity should decrease. Several studies show that copper is non-cytotoxic, while Ag-NPs seem to have a higher toxicity (75, 80-82).

5 CONCLUSION

We were able to synthesise the copper and silver nanoparticles by using extracts of two different species of blueberry as a reducing agent.

Size and structure of the metal nanoparticles were characterised by TEM analysis and found acceptable. Moreover, we confirmed that the conditions applied during the synthesis have an effect on the size and structure of nanoparticles

However, our copper nanoparticles did not show antibacterial effect in our study, probably due to their instability and tendency to aggregate. Our silver nanoparticles did exhibit an antibacterial effect; however, it was not greater than, or equal to, the antibacterial effect of the silver nitrate solution alone. More experiments where synthesis of nanoparticles is performed with different concentrations of metal precursor and extract to optimize a composition assuring a more stable nanoparticle suspension. Another possibility is to make the synthesis in the presence of biocompatible molecules, which can be absorbed on the nanoparticle surface while stabilizing the suspension by electrostatic repulsions. For this purpose a good candidate is the citrate ions, which can be obtained in large quantities from plant extracts, thus complying to green chemistry requirements.

All the nanoparticle suspensions showed toxicity toward keratinocytes in toxicity assay. This is however not conclusive evidence for their toxicity since the suspensions very unstable, causing the nanoparticles and extracts to aggregate and precipitate. Toxicity testing should be repeated when a more stable suspension of the nanoparticles has been prepared.

6 FUTURE PERSPECTIVES

In this study we prepared copper and silver nanoparticles by using extracts of blueberries (*V. myrtillus* and *V. gaultherioides*) as a reducing and capping agent. Green chemistry criteria (low temperatures, non toxic solvents, etc.) were also followed in the process.

The nanoparticles synthesised exhibited no (Cu-NPs) or low (Ag-NPs) antibacterial effect, respectively, and all of them exhibited high toxicity towards keratinocytes. This is believed to mainly be caused by a tendency of the nanoparticle suspensions to aggregate and precipitate. Therefore, the main focus of future experiments should be on optimizing a composition and synthesis procedure to obtain a more stable nanoparticle suspensions. This should be possible by varying the concentration of extract and metal precursor salt. Another possibility would be to add other biocompatible molecules to help stabilize the suspension. One of these molecules could be citrate ions, which are obtainable in large quantities from plant extracts, which means the principles of green chemistry are still being followed.

A way to properly determine how much nanoparticles are synthesised and reaction speed should be applied. UV-vis spectrometry has been reported in several other studies as a way to do this; and it might be easier to do this once a synthesis with a more diluted extract is used, causing less interference of the absorption spectra by the extract itself and making it easier to find a peak absorbance that can be attributed to the copper and silver nanoparticles alone.

Antibacterial testing and toxicity assays should be repeated when a more stable suspension of nanoparticles is prepared. For antibacterial testing, it might be suitable to use a method that makes it comparable to other studies and experiments (e.g. broth dilution assay on microtiter plates or antibacterial testing in agitated liquid medium). If the suspension is more stable, using the disk diffusion test might be possible too.

Reference list

1. Silver LL. Challenges of antibacterial discovery. Clinical Microbiology Reviews. 2011;24(1):71-109.
2. Huh AJ, Kwon YJ. "Nanoantibiotics": a new paradigm for treating infectious diseases using nanomaterials in the antibiotics resistant era. Journal of Controlled Release. 2011;156(2):128-45.
3. WHO. Antimicrobial resistance: global report on surveillance 2014. who.int; 2014 April 2014.
4. Shata MT, Stevceva L, Agwale S, Lewis GK, Hone DM. Recent advances with recombinant bacterial vaccine vectors. Molecular Medicine Today. 2000;6(2):66-71.
5. Kreuter J. Liposomes and nanoparticles as vehicles for antibiotics. Infection. 1991;19:S224-S8.
6. Petros RA, DeSimone JM. Strategies in the design of nanoparticles for therapeutic applications. Nature Reviews Drug discovery. 2010;9(8):615-27.
7. Allen TM, Cullis PR. Drug delivery systems: entering the mainstream. Science (New York, NY). 2004;303(5665):1818-22.
8. Drake PL, Hazelwood KJ. Exposure-related health effects of silver and silver compounds: a review. Annals of Occupational Hygiene. 2005;49(7):575-85.
9. Blanc D, Carrara P, Zanetti G, Francioli P. Water disinfection with ozone, copper and silver ions, and temperature increase to control Legionella: seven years of experience in a university teaching hospital. Journal of Hospital Infection. 2005;60(1):69-72.
10. Esteban-Tejeda L, Malpartida F, Esteban-Cubillo A, Pecharromán C, Moya J. Antibacterial and antifungal activity of a soda-lime glass containing copper nanoparticles. Nanotechnology. 2009;20(50):505701.
11. Long TC, Saleh N, Tilton RD, Lowry GV, Veronesi B. Titanium dioxide (P25) produces reactive oxygen species in immortalized brain microglia (BV2): implications for nanoparticle neurotoxicity. Environmental Science & Technology. 2006;40(14):4346-52.
12. Panyala NR, Peña-Méndez EM, Havel J. Silver or silver nanoparticles: a hazardous threat to the environment and human health. Journal of Applied Biomedicine. 2008;6(3):117-29.
13. Fabrega J, Luoma SN, Tyler CR, Galloway TS, Lead JR. Silver nanoparticles: behaviour and effects in the aquatic environment. Environment International. 2011;37(2):517-31.
14. Griffitt RJ, Weil R, Hyndman KA, Denslow ND, Powers K, Taylor D, et al. Exposure to copper nanoparticles causes gill injury and acute lethality in zebrafish (Danio rerio). Environmental Science & Technology. 2007;41(23):8178-86.
15. Borkow G, Gabbay J. Copper, an ancient remedy returning to fight microbial, fungal and viral infections. Current Chemical Biology. 2009;3(3):272-8.
16. Borkow G, Gabbay J. Copper as a biocidal tool. Current Medicinal Chemistry. 2005;12(18):2163-75.
17. Wilks SA, Michels HT, Keevil CW. Survival of Listeria monocytogenes Scott A on metal surfaces: implications for cross-contamination. International Journal of Food Microbiology. 2006;111(2):93-8.
18. Uauy R, Olivares M, Gonzalez M. Essentiality of copper in humans. The American Journal of Clinical Nutrition. 1998;67(5):952S-9S.
19. Borkow G, Gabbay J, Zatcoff RC. Could chronic wounds not heal due to too low local copper levels? Medical Hypotheses. 2008;70(3):610-3.
20. Cachafeiro SP, Naveira IM, García IG. Is copper–silver ionisation safe and effective in controlling legionella? Journal of Hospital Infection. 2007;67(3):209-16.
21. Mott D, Galkowski J, Wang L, Luo J, Zhong C-J. Synthesis of size-controlled and shaped copper nanoparticles. Langmuir. 2007;23(10):5740-5.
22. Lee HJ, Song JY, Kim BS. Biological synthesis of copper nanoparticles using Magnolia kobus leaf extract and their antibacterial activity. Journal of Chemical Technology and Biotechnology. 2013;88(11):1971-7.
23. Mittu R. Synthesis, Characterization of Copper Nanoparticles-A Review. Synthesis. 2016;3(5).

24. Haverkamp RG, Marshall AT, van Agterveld D. Pick your carats: nanoparticles of gold–silver–copper alloy produced in vivo. Journal of Nanoparticle Research. 2007;9(4):697-700.
25. Yallappa S, Manjanna J, Sindhe M, Satyanarayan N, Pramod S, Nagaraja K. Microwave assisted rapid synthesis and biological evaluation of stable copper nanoparticles using T. arjuna bark extract. Spectrochimica Acta Part A: Molecular and Biomolecular Spectroscopy. 2013;110:108-15.
26. Chandran SP, Chaudhary M, Pasricha R, Ahmad A, Sastry M. Synthesis of Gold Nanotriangles and Silver Nanoparticles Using Aloevera Plant Extract. Biotechnology Progress. 2006;22(2):577-83.
27. Mittal AK, Chisti Y, Banerjee UC. Synthesis of metallic nanoparticles using plant extracts. Biotechnology Advances. 2013;31(2):346-56.
28. Christian P, Von der Kammer F, Baalousha M, Hofmann T. Nanoparticles: structure, properties, preparation and behaviour in environmental media. Ecotoxicology. 2008;17(5):326-43.
29. Auffan M, Rose J, Bottero J-Y, Lowry GV, Jolivet J-P, Wiesner MR. Towards a definition of inorganic nanoparticles from an environmental, health and safety perspective. Nature Nanotechnology. 2009;4(10):634-41.
30. Clark JH. Green chemistry: challenges and opportunities. Green Chemistry. 1999;1(1):1-8.
31. Constable DJ, Dunn PJ, Hayler JD, Humphrey GR, Leazer Jr JL, Linderman RJ, et al. Key green chemistry research areas—a perspective from pharmaceutical manufacturers. Green Chemistry. 2007;9(5):411-20.
32. Anastas PT, Warner JC. Principles of green chemistry. Green chemistry: Theory and practice. 1998:29-56.
33. Duan H, Wang D, Li Y. Green chemistry for nanoparticle synthesis. Chemical Society Reviews. 2015;44(16):5778-92.
34. Blåbær - slik lykkes du. In: myrtillus V, editor. http://www.plantasjen.no/ Plantasjen; 2016.
35. Vaccinium gaultherioides. In: gaultherioides V, editor. http://botanische-spaziergaenge.at/ Botanische-Spaziergaenge; 2010.
36. Ancillotti C, Ciofi L, Pucci D, Sagona E, Giordani E, Biricolti S, et al. Polyphenolic profiles and antioxidant and antiradical activity of Italian berries from Vaccinium myrtillus L. and Vaccinium uliginosum L. subsp. gaultherioides (Bigelow) SB Young. Food Chemistry. 2016;204:176-84.
37. Janeiro P, Brett AMO. Redox Behavior of Anthocyanins Present in Vitis vinifera L. Electroanalysis. 2007;19(17):1779-86.
38. Arroyo-Currás N, Videa MF. Electrochemical Study of Flavonoids in Acetonitrile: Structure-Activity Relationships. ECS Transactions. 2010;29(1):349-59.
39. Durán N, Marcato PD, De Souza GI, Alves OL, Esposito E. Antibacterial effect of silver nanoparticles produced by fungal process on textile fabrics and their effluent treatment. Journal of Biomedical Nanotechnology. 2007;3(2):203-8.
40. Rai M, Yadav A, Gade A. Silver nanoparticles as a new generation of antimicrobials. Biotechnology Advances. 2009;27(1):76-83.
41. Rosenman KD, Moss A, Kon S. Argyria: clinical implications of exposure to silver nitrate and silver oxide. Journal of Occupational and Environmental Medicine. 1979;21(6):430-5.
42. Prabhu S, Poulose EK. Silver nanoparticles: mechanism of antimicrobial action, synthesis, medical applications, and toxicity effects. International Nano Letters. 2012;2(1):32.
43. Cohen SY, Quentel G, Egasse D, Cadot M, Ingster-moati I, Coscas GJ. The dark choroid in systemic argyrosis. Retina. 1993;13(4):302-6.
44. Yoon K-Y, Byeon JH, Park J-H, Hwang J. Susceptibility constants of Escherichia coli and Bacillus subtilis to silver and copper nanoparticles. Science of the Total Environment. 2007;373(2):572-5.
45. Ruparelia JP, Chatterjee AK, Duttagupta SP, Mukherji S. Strain specificity in antimicrobial activity of silver and copper nanoparticles. Acta Biomaterialia. 2008;4(3):707-16.
46. Zain NM, Stapley A, Shama G. Green synthesis of silver and copper nanoparticles using ascorbic acid and chitosan for antimicrobial applications. Carbohydrate Polymers. 2014;112:195-202.
47. Liau S, Read D, Pugh W, Furr J, Russell A. Interaction of silver nitrate with readily identifiable groups: relationship to the antibacterialaction of silver ions. Letters in Applied Microbiology. 1997;25(4):279-83.

48. Feng Q, Wu J, Chen G, Cui F, Kim T, Kim J. A mechanistic study of the antibacterial effect of silver ions on Escherichia coli and Staphylococcus aureus. Journal of Biomedical Materials Research. 2000;52(4):662-8.
49. Song H, Ko K, Oh I, Lee B. Fabrication of silver nanoparticles and their antimicrobial mechanisms. European Cells & Materials Journal. 2006;11(Suppl 1):58.
50. Morones JR, Elechiguerra JL, Camacho A, Holt K, Kouri JB, Ramírez JT, et al. The bactericidal effect of silver nanoparticles. Nanotechnology. 2005;16(10):2346.
51. Castellano JJ, Shafii SM, Ko F, Donate G, Wright TE, Mannari RJ, et al. Comparative evaluation of silver‐containing antimicrobial dressings and drugs. International Wound Journal. 2007;4(2):114-22.
52. Yashroy R. Lamellar dispersion and phase separation of chloroplast membrane lipids by negative staining electron microscopy. Journal of Biosciences. 1990;15(2):93-8.
53. Eccles D. Scheme_TEM_en. In: Scheme_TEM_en, editor. http://www.en.wikipedia.org2009/.
54. Engelkirk PG, Duben-Engelkirk JL. Laboratory diagnosis of infectious diseases: essentials of diagnostic microbiology: Lippincott Williams & Wilkins; 2008.
55. Tripathi K. Essentials of medical pharmacology: JP Medical Ltd; 2013.
56. Bauer AW, Kirby WM, Sherris JC, Turck M. Antibiotic susceptibility testing by a standardized single disk method. American Journal of Clinical Pathology. 1966;45(4):493-6.
57. Vistica DT, Skehan P, Scudiero D, Monks A, Pittman A, Boyd MR. Tetrazolium-based assays for cellular viability: a critical examination of selected parameters affecting formazan production. Cancer Research. 1991;51(10):2515-20.
58. Slater T, Sawyer B, Sträuli U. Studies on succinate-tetrazolium reductase systems: III. Points of coupling of four different tetrazolium salts III. Points of coupling of four different tetrazolium salts. Biochimica et Biophysica Acta. 1963;77:383-93.
59. Maehara Y, Anai H, Tamada R, Sugimachi K. The ATP assay is more sensitive than the succinate dehydrogenase inhibition test for predicting cell viability. European Journal of Cancer and Clinical Oncology. 1987;23(3):273-6.
60. Berridge MV, Tan AS. Characterization of the Cellular Reduction of 3-(4,5-dimethylthiazol-2-yl)-2,5-diphenyltetrazolium bromide (MTT): Subcellular Localization, Substrate Dependence, and Involvement of Mitochondrial Electron Transport in MTT Reduction. Archives of biochemistry and biophysics. 1993;303(2):474-82.
61. LB (Luria-Bertani) liquid medium. Cold Spring Harbor Protocols. 2006;2006(1):pdb.rec8141.
62. Media containing agar or agarose. Cold Spring Harbor Protocols. 2006;2006(1):pdb.rec8734.
63. Padil VVT, Černík M. Green synthesis of copper oxide nanoparticles using gum karaya as a biotemplate and their antibacterial application. International Journal of Nanomedicine. 2013.
64. Kobayashi Y, Sakuraba T. Silica-coating of metallic copper nanoparticles in aqueous solution. Colloids and Surfaces A: Physicochemical and Engineering Aspects. 2008;317(1):756-9.
65. Ramyadevi J, Jeyasubramanian K, Marikani A, Rajakumar G, Rahuman AA. Synthesis and antimicrobial activity of copper nanoparticles. Materials Letters. 2012;71:114-6.
66. Inaba M. Tarnishing of silver: a short review. V&A Conservation Journal. 1996(18):9-10.
67. Rogers D. The chemistry of photography: from classical to digital technologies: Royal Society of Chemistry; 2007.
68. Araujo R. Photochromism in glasses containing silver halides. Contemporary Physics. 1980;21(1):77-84.
69. Lee Y, Choi J-r, Lee KJ, Stott NE, Kim D. Large-scale synthesis of copper nanoparticles by chemically controlled reduction for applications of inkjet-printed electronics. Nanotechnology. 2008;19(41):415604.
70. Kobayashi Y, Shirochi T, Yasuda Y, Morita T. Preparation of metallic copper nanoparticles in aqueous solution and their bonding properties. Solid State Sciences. 2011;13(3):553-8.
71. Kobayashi Y, Ishida S, Ihara K, Yasuda Y, Morita T, Yamada S. Synthesis of metallic copper nanoparticles coated with polypyrrole. Colloid and Polymer Science. 2009;287(7):877-80.
72. Volf I, Ignat I, Neamtu M, Popa VI. Thermal stability, antioxidant activity, and photo-oxidation of natural polyphenols. Chemical Papers. 2014;68(1):121-9.

73. Bkowska A, Kucharska AZ, Oszmiański J. The effects of heating, UV irradiation, and storage on stability of the anthocyanin–polyphenol copigment complex. Food Chemistry. 2003;81(3):349-55.
74. Ross CF, Hoye Jr C, Fernandez‐Plotka VC. Influence of heating on the polyphenolic content and antioxidant activity of grape seed flour. Journal of Food Science. 2011;76(6):C884-C90.
75. Valodkar M, Nagar PS, Jadeja RN, Thounaojam MC, Devkar RV, Thakore S. Euphorbiaceae latex induced green synthesis of non-cytotoxic metallic nanoparticle solutions: a rational approach to antimicrobial applications. Colloids and Surfaces A: Physicochemical and Engineering Aspects. 2011;384(1):337-44.
76. Gabbay J, Borkow G, Mishal J, Magen E, Zatcoff R, Shemer-Avni Y. Copper oxide impregnated textiles with potent biocidal activities. Journal of Industrial Textiles. 2006;35(4):323-35.
77. Shahrokh S, Emtiazi G. Toxicity and unusual biological behavior of nanosilver on gram positive and negative bacteria assayed by microtiter-plate. European Journal of Biological Sciences. 2009;1(3):28-31.
78. Premanathan M, Karthikeyan K, Jeyasubramanian K, Manivannan G. Selective toxicity of ZnO nanoparticles toward Gram-positive bacteria and cancer cells by apoptosis through lipid peroxidation. Nanomedicine: Nanotechnology, Biology and Medicine. 2011;7(2):184-92.
79. Choi O, Deng KK, Kim N-J, Ross L, Surampalli RY, Hu Z. The inhibitory effects of silver nanoparticles, silver ions, and silver chloride colloids on microbial growth. Water Research. 2008;42(12):3066-74.
80. Valodkar M, Rathore PS, Jadeja RN, Thounaojam M, Devkar RV, Thakore S. Cytotoxicity evaluation and antimicrobial studies of starch capped water soluble copper nanoparticles. Journal of Hazardous Materials. 2012;201:244-9.
81. AshaRani P, Low Kah Mun G, Hande MP, Valiyaveettil S. Cytotoxicity and genotoxicity of silver nanoparticles in human cells. ACS Nano. 2008;3(2):279-90.
82. Asharani P, Wu YL, Gong Z, Valiyaveettil S. Toxicity of silver nanoparticles in zebrafish models. Nanotechnology. 2008;19(25):255102.

Appendix

Microtiter Plates

Table 14 - *E. coli* ATCC 35218 plate 1. $CuCl_2$ and $Cu(CH_3COO)_2$ synthesised at 70 °C. Metal concentration $2.5*10^{-2}$, undiluted extract.

<>	1	2	3	4	5	6	7	8	9	10	11	12
A	1,123	1,050	1,322	1,308	1,232	1,170	1,147	1,116	1,104	1,112	1,100	1,136
B	1,066	1,064	1,225	1,189	1,202	1,141	1,127	1,064	1,078	1,044	1,082	1,027
C	1,315	0,888	1,207	1,179	1,199	1,111	1,116	1,099	1,079	1,053	1,072	1,051
D	0,830	1,257	1,490	1,338	1,169	1,096	1,102	1,067	1,029	1,035	1,039	1,030
E	0,737	1,283	1,482	1,321	1,172	1,104	1,087	1,063	1,056	1,043	1,040	1,042
F	1,535	1,000	1,349	1,209	1,196	1,150	1,107	1,093	1,078	1,081	1,072	1,062
G	1,519	0,911	1,411	1,218	1,185	1,137	1,112	1,097	1,074	1,095	1,077	1,057
H	0,999	1,071	1,418	1,281	1,224	1,168	1,138	1,117	1,096	1,115	1,103	1,137

Table 15 - Overview of samples in plate in Table 14

	1
A	$CuCl_2$ + M
B	$CuCl_2$ + M
C	$CuCl_2$ + M
D	*myrtillus* extract
E	*myrtillus* extract
F	$Cu(CH_3COO)_2$ + M
G	$Cu(CH_3COO)_2$ + M
H	$Cu(CH_3COO)_2$ + M

Table 16 - *E. coli* ATCC 35218 plate 2. $CuCl_2$ and $Cu(CH_3COO)_2$ synthesised at 70°C. Metal concentration $2.5*10^{-2}$, undiluted extract.

<>	1	2	3	4	5	6	7	8	9	10	11	12
A	0,658	1,217	1,425	1,341	1,179	1,211	1,182	1,189	1,184	1,213	1,231	0,144
B	0,565	1,068	1,355	1,256	1,194	1,214	1,177	1,165	1,161	1,180	1,204	0,172
C	0,536	0,968	1,297	1,248	1,207	1,186	1,177	1,163	1,168	1,172	1,193	1,040
D	1,074	1,183	1,397	1,311	1,217	1,225	1,173	1,159	1,155	1,158	1,183	0,177
E	1,088	1,194	1,403	1,350	1,206	1,215	1,164	1,157	1,154	1,156	1,184	1,043
F	0,650	0,975	1,363	1,283	1,256	1,226	1,192	1,171	1,165	1,184	1,212	0,190
G	0,629	1,049	1,413	1,267	1,184	1,182	1,179	1,152	1,168	1,190	1,200	0,189
H	0,938	1,181	1,449	1,369	1,245	1,209	1,191	1,184	1,182	1,212	1,221	0,229

Table 17 - Overview of samples in plate in Table 22

	1
A	$CuCl_2$ + G
B	$CuCl_2$ + G
C	$CuCl_2$ + G
D	*gaultherioides* extract
E	*gaultherioides* extract
F	$Cu(CH_3COO)_2$ + G
G	$Cu(CH_3COO)_2$ + G
H	$Cu(CH_3COO)_2$ + G

Table 18 - *S. aureus* ATCC 25923 plate 1. $CuCl_2$ and $Cu(CH_3COO)_2$ synthesised at 70 ^oC. Metal concentration $2.5*10^{-2}$, undiluted extract.

<>	1	2	3	4	5	6	7	8	9	10	11	12
A	1,387	0,413	0,399	0,445	0,532	0,353	0,417	0,431	0,537	0,500	0,555	0,589
B	1,191	0,483	0,475	0,507	0,651	0,625	0,577	0,414	0,430	0,397	0,375	0,518
C	1,398	0,528	0,481	0,721	0,796	0,463	0,461	0,402	0,503	0,382	0,395	0,385
D	0,763	0,754	0,431	0,865	0,942	0,726	0,570	0,404	0,430	0,382	0,380	0,395
E	0,925	0,800	0,456	0,763	0,704	0,474	0,370	0,409	0,397	0,384	0,397	0,452
F	1,619	0,806	0,521	0,510	0,646	0,593	0,580	0,483	0,599	0,432	0,337	0,396
G	1,448	0,810	0,519	0,603	0,602	0,595	0,469	0,582	0,392	0,465	0,362	0,446
H	1,558	1,140	0,483	0,486	0,582	0,458	0,394	0,359	0,517	0,483	0,555	0,692

Table 19 - Overview of samples in plate in Table 18

	1
A	$CuCl_2$ + M
B	$CuCl_2$ + M
C	$CuCl_2$ + M
D	*myrtillus* extract
E	*myrtillus* extract
F	$Cu(CH_3COO)_2$ + M
G	$Cu(CH_3COO)_2$ + M
H	$Cu(CH_3COO)_2$ + M

Table 20 - *S. aureus* ATCC 25923 plate 2. $CuCl_2$ and $Cu(CH_3COO)_2$ synthesised at 70 °C. Metal concentration $2.5*10^{-2}$, undiluted extract.

<>	1	2	3	4	5	6	7	8	9	10	11	12
A	0,773	0,320	0,385	0,395	0,355	0,368	0,432	0,438	0,451	0,420	0,417	0,090
B	0,749	0,319	0,414	0,376	0,494	0,457	0,293	0,297	0,300	0,266	0,266	0,106
C	0,697	0,324	0,391	0,447	0,440	0,487	0,360	0,278	0,270	0,271	0,269	0,099
D	0,197	0,392	0,344	0,317	0,284	0,280	0,277	0,255	0,268	0,263	0,262	0,099
E	0,251	0,342	0,397	0,310	0,284	0,283	0,294	0,267	0,269	0,258	0,286	0,109
F	0,888	0,491	0,428	0,358	0,323	0,410	0,292	0,293	0,286	0,275	0,265	0,115
G	0,824	0,390	0,464	0,371	0,438	0,429	0,443	0,302	0,285	0,296	0,295	0,360
H	0,648	0,584	0,451	0,375	0,643	0,392	0,523	0,390	0,527	0,416	0,435	0,089

Table 21 - Overview of samples in plate in Table 20

	1
A	$CuCl_2$ + G
B	$CuCl_2$ + G
C	$CuCl_2$ + G
D	*gaultherioides* extract
E	*gaultherioides* extract
F	$Cu(CH_3COO)_2$ + G
G	$Cu(CH_3COO)_2$ + G
H	$Cu(CH_3COO)_2$ + G

Table 22 - *E. coli* ATCC 35218. Copper and silver nitrate synthesised at 50°C. Metal concentration in original sample: $1,25*10^{-2}$, extract diluted 1:1.

<>	1	2	3	4	5	6	7	8	9	10	11	12
A	1,191	1,312	1,072	0,986	0,940	0,910	0,903	0,893	0,865	0,893	0,910	0,048
B	1,011	1,129	1,005	0,955	0,913	0,894	0,857	0,838	0,819	0,837	0,870	0,048
C	0,548	0,908	0,950	0,886	0,869	0,871	0,883	0,845	0,869	0,858	0,864	0,838
D	0,782	0,274	0,194	0,134	0,090	0,453	0,676	0,752	0,760	0,780	0,815	0,854
E	0,253	0,855	0,890	0,884	0,866	0,882	0,929	0,895	0,863	0,849	0,854	0,608
F	0,310	0,275	0,178	0,124	0,094	0,072	0,602	0,733	0,757	0,775	0,816	0,379
G	0,557	0,657	0,719	0,803	0,861	0,927	0,918	0,886	0,886	0,847	0,887	0,919
H	0,087	0,076	0,064	0,059	0,056	0,053	0,471	0,837	0,836	0,840	0,868	1,597

Table 23 - Overview of samples in plate in Table 22.

	1	12
A	M	Positive control
B	G	Positive control
C	CuNO3 + M	Negative control
D	AgNO3 + M	Negative control
E	CuNO3 + G	M extract
F	AgNO3 + G	G extract
G	CuNO3 1.25	CuNO3 + M
H	AgNO3 1.25	AgNO3 + M

Table 24 - *S. aureus* ATCC 25923. Copper and silver nitrate synthesised at 50^{o}C. Metal concentration in original sample: 1.25*10^{-2}, extract diluted 1:1.

<>	1	2	3	4	5	6	7	8	9	10	11	12
A	0,317	0,328	0,298	0,423	0,443	0,554	0,638	0,648	0,879	0,992	0,892	0,062
B	0,277	0,298	0,261	0,267	0,283	0,342	0,244	0,400	0,417	0,743	0,654	0,048
C	0,762	0,419	0,463	0,414	0,724	0,646	0,870	0,501	0,722	0,941	0,755	0,921
D	0,756	0,202	0,605	0,093	0,080	0,066	0,090	0,553	0,376	0,513	0,503	0,836
E	0,185	0,276	0,510	0,481	0,984	0,999	0,651	0,800	0,727	0,768	0,746	0,067
F	0,293	0,233	0,159	0,097	0,072	0,064	0,440	0,202	0,383	0,433	0,522	0,050
G	0,598	1,042	0,553	0,870	0,822	1,013	0,896	0,916	0,827	0,825	0,662	0,048
H	0,069	0,061	0,060	0,056	0,056	0,053	0,150	0,253	0,744	0,885	0,892	0,045

Table 25 – Overview of samples in plate in Table 24.

	1	12
A	M	Positive control
B	G	Positive control
C	$CuNO_3$ + M	Negative controls
D	$AgNO_3$ + M	
E	$CuNO_3$ + G	
F	$AgNO_3$ + G	
G	$CuNO_3$ 1.25 M	
H	$AgNO_3$ 1.25 M	

Table 26 - *S. aureus* ATCC 29213. Copper and silver nitrate synthesised at 50°C. Metal concentration in original sample: $1.25*10^{-2}$, extract diluted 1:1.

<>	1	2	3	4	5	6	7	8	9	10	11	12
A	0,306	0,387	0,879	0,842	0,932	0,830	0,821	0,749	0,751	0,724	0,712	0,049
B	0,356	0,340	0,833	1,076	1,040	0,889	0,876	0,730	0,601	0,596	0,613	0,048
C	0,429	0,569	0,661	0,949	0,824	0,685	0,768	0,647	0,600	0,701	0,599	0,741
D	0,662	0,210	0,162	0,113	0,082	0,131	0,525	0,558	0,587	0,754	0,589	0,797
E	0,168	0,299	0,983	0,945	0,813	0,607	0,712	0,567	0,689	0,554	0,696	0,574
F	0,424	0,221	0,142	0,093	0,074	0,418	0,585	0,779	0,658	0,593	0,608	0,536
G	0,138	0,547	0,662	0,674	0,619	0,651	0,549	0,669	0,651	0,636	0,572	0,116
H	0,058	0,056	0,061	0,057	0,060	0,053	0,510	0,623	0,768	0,770	0,824	0,071

Table 27 – Overview of samples in plate in Table 26

	1	12
A	M	Positive control
B	G	Positive control
C	CuNO3 + M	Negative control
D	AgNO3 + M	Negative control
E	CuNO3 + G	CuNO3 + G
F	AgNO3 + G	AgNO3 + G
G	CuNO3 1.25 M	CuNO3 1.25 M
H	AgNO3 1.25 M	AgNO3 1.25 M

Table 28 - *E. coli* ATCC 35218 plate 1. $AgNO_3$ $1.25*10^{-2}$M, extract diluted 1:1, and $2.5*10^{-2}$M with undiluted extract, synthesised at 70°C.

<>	1	2	3	4	5	6	7	8	9	10	11	12
A	1,695	1,276	1,126	1,053	0,990	0,956	0,945	0,950	0,954	0,947	0,965	0,873
B	1,508	1,291	1,114	1,037	0,965	0,948	0,921	0,894	0,886	0,897	0,948	0,043
C	1,513	1,312	1,107	1,050	0,974	0,926	0,883	0,884	0,863	0,891	0,920	0,043
D	1,179	1,426	1,350	1,099	1,040	0,981	0,914	0,925	0,902	0,923	0,928	0,911
E	2,187	1,951	1,046	0,545	0,350	0,220	0,146	0,088	0,126	0,050	0,700	0,886
F	1,251	0,616	0,247	0,141	0,098	0,082	0,835	0,890	0,899	0,863	0,878	0,912
G	1,208	0,437	0,224	0,139	0,095	0,074	0,830	0,878	0,878	0,869	0,899	0,876
H	1,401	0,875	0,223	0,132	0,100	0,073	0,855	0,904	0,895	0,894	0,970	1,999

Table 29 - Overview of samples in plate in Table 28

	1	12
A	Ag 1.25 + M1/2	Negative control
B	Ag 1.25 + M1/2	Negative control
C	Ag 1.25 + M1/2	Negative control
D	*myrtillus* extract	Positive control
E	$AgNO_3$ 2.5*10^-2	Positive control
F	$AgNO_3$ 2.5 + M1/1	Positive control
G	$AgNO_3$ 2.5 + M1/1	*myrtillus*
H	$AgNO_3$ 2.5 + M1/1	$AgNO_3$ 2.5*10^-2

Table 30 - *E. coli* ATCC 35218 plate 2. $AgNO_3$ 1.25*10^{-2}M, extract diluted 1:1, and 2.5*10^{-2}M with undiluted extract, synthesised at 70^{o}C.

<>	1	2	3	4	5	6	7	8	9	10	11	12
A	0,301	0,198	0,146	0,091	0,068	0,737	0,928	0,946	0,935	0,910	0,916	0,043
B	0,307	0,181	0,131	0,089	0,064	0,831	0,907	0,927	0,892	0,874	0,881	0,821
C	0,304	0,190	0,136	0,094	0,138	0,771	0,893	0,897	0,882	0,896	0,877	0,043
D	1,239	1,043	1,263	1,099	1,052	1,011	0,979	0,940	0,929	0,909	0,914	0,941
E	1,635	1,072	0,663	0,416	0,271	0,187	0,120	0,056	0,048	0,716	0,848	0,941
F	0,923	0,255	0,167	0,116	0,082	0,064	0,864	0,935	0,905	0,887	0,891	0,938
G	0,891	0,274	0,169	0,122	0,153	0,068	0,878	0,912	0,896	0,938	0,917	0,333
H	1,200	0,317	0,162	0,113	0,082	0,067	0,770	0,930	0,928	0,908	0,957	1,160

Table 31 - Overview of samples in plate in Table 30

	1	12
A	Ag 1.25 + G1/2	Negative control
B	Ag 1.25 + G1/2	Negative control
C	Ag 1.25 + G1/2	Negative control
D	*gaultherioides* extract	Positive control
E	Ag 2.5*10^-2	Positive control
F	Ag 2.5 + G1/1	Positive control
G	Ag 2.5 + G1/1	M + Ag 1.25
H	Ag 2.5 + G1/1	M + Ag 2.5

Table 32 - *S.aureus* ATCC 25923 plate 1. $AgNO_3$ 1.25*10^{-2}M, extract diluted 1:1, and 2.5*10^{-2}M with undiluted extract, synthesised at 70°C.

<>	1	2	3	4	5	6	7	8	9	10	11	12
A	0,662	0,611	0,470	0,736	0,815	0,831	0,896	0,905	0,713	0,822	0,870	0,139
B	0,396	0,322	0,340	0,280	0,320	0,314	0,284	0,541	0,343	0,349	0,287	0,044
C	0,366	0,324	0,309	0,293	0,273	0,274	0,202	0,378	0,298	0,261	0,211	0,044
D	0,629	0,340	0,340	0,337	0,353	0,308	0,262	0,338	0,332	0,397	0,201	0,273
E	2,230	1,803	0,854	0,481	0,303	0,194	0,121	0,077	0,062	0,071	0,119	0,276
F	0,925	0,528	0,203	0,128	0,105	0,096	0,197	0,349	0,256	0,199	0,251	0,342
G	1,101	0,592	0,194	0,126	0,097	0,085	0,191	0,348	0,344	0,269	0,305	0,568
H	1,225	0,787	0,202	0,122	0,092	0,099	0,229	0,480	0,619	0,557	0,561	2,114

Table 33 – Overview of samples in plate in Table 32

	1	12
A	Ag 1.25 + M1/2	Negative control
B	Ag 1.25 + M1/2	Negative control
C	Ag 1.25 + M1/2	Negative control
D	*myrtillus* extract	Positive control
E	Ag 2.5*10^-2	Positive control
F	Ag 2.5 + M1/1	Positive control
G	Ag 2.5 + M1/1	*myrtillus*
H	Ag 2.5 + M1/1	Ag 2.5*10^-2

Table 34 - *S. Aureus* ATCC 25923 plate 2. $AgNO_3$ 1.25*10^{-2}M, extract diluted 1:1, and 2.5*10^{-2}M with undiluted extract, synthesised at 70°C.

<>	1	2	3	4	5	6	7	8	9	10	11	12
A	0,255	0,195	0,138	0,098	0,072	0,134	0,210	0,607	0,877	0,771	0,721	0,045
B	0,282	0,200	0,161	0,105	0,086	0,123	0,206	0,253	0,309	0,229	0,289	0,043
C	0,298	0,280	0,161	0,092	0,080	0,140	0,199	0,250	0,322	0,185	0,191	0,044
D	0,308	0,322	0,252	0,290	0,292	0,312	0,259	0,230	0,214	0,190	0,201	0,237
E	1,383	0,802	0,363	0,195	0,138	0,093	0,072	0,058	0,085	0,134	0,215	0,269
F	1,020	0,224	0,152	0,107	0,097	0,074	0,160	0,218	0,209	0,198	0,306	0,304
G	1,139	0,249	0,172	0,126	0,087	0,073	0,199	0,215	0,205	0,222	0,314	0,575
H	1,096	0,280	0,159	0,099	0,094	0,068	0,153	0,205	0,502	0,570	0,473	1,416

Table 35 - Overview of samples in plate in Table 34

	1	12
A	Ag 1.25 + G1/2	Negative control
B	Ag 1.25 + G1/2	Negative control
C	Ag 1.25 + G1/2	Negative control
D	*gaultherioides* extract	Positive control
E	Ag 2.5*10^-2	Positive control
F	Ag 2.5 + G1/1	Positive control
G	Ag 2.5 + G1/1	M + Ag 1.25 M
H	Ag 2.5 + G1/1	M + Ag 2.5 M